

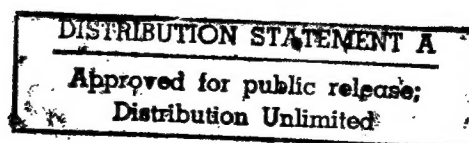


JPRS Report

Science & Technology

USSR: Physics & Mathematics

19990210 029



DTIC QUALITY INSPECTED 3

REPRODUCED BY
U.S. DEPARTMENT OF COMMERCE
NATIONAL TECHNICAL
INFORMATION SERVICE
SPRINGFIELD, VA 22161

DTIC QUALITY INSPECTED 2

Science & Technology

USSR: Physics & Mathematics

JPRS-UPM-91-006

CONTENTS

16 September 1991

Acoustics

- Nonlinear Dynamics and Abnormal Electroacoustic Wave Attenuation in Order-Disorder Ferroelectrics
 [M. B. Belonenko, M. M. Shakirzyanov; *ZHURNAL EKSPERIMENTALNOY I TEORETICHESKOY FIZIKI* Vol 99 No 3, Mar 91] 1
- Speed of Sound in He-CO₂ Mixtures Under High Pressures
 [L. I. Pitayevskaya, A. A. Popov; *DOKLADY AKADEMII NAUK SSSR* Vol 316 No 5, Feb 91] 1
- Cumulation Effect During Interaction of Standing Shock Wave and Conical Body
 [Yu. M. Beletskiy, D. F. Bykov, et al.; *PISMA V ZHURNAL TEKHNIЧЕСКОY FIZIKI* Vol 17 No 5, 12 Mar 91] 1
- Shock Waves in Developing Gas Discharge
 [Yu. I. Chutov, V. N. Podolskiy, et al.; *PISMA V ZHURNAL TEKHNIЧЕСКОY FIZIKI* Vol 17 No 3, 12 Feb 91] 2
- Relativistic Electron Beam Propagation in Extragalactic Jet Plasma in Gas Dynamic Approximation
 [V. M. Melnik; *UKRAINSKIY FIZICHESKIY ZHURNAL* Vol 36 No 3, Mar 91] 2

Crystals, Laser Glasses, Semiconductors

- Solitons in Charge Density Wave Crystals
 [S. A. Brazovskiy, S. I. Matveyenko; *ZHURNAL EKSPERIMENTALNOY I TEORETICHESKOY FIZIKI* Vol 99 No 3, Mar 91] 3
- Electrophysical Properties of HfNi_{1-x}Co_xSn (0 ≤ x ≤ 0.4) Compounds
 [A. O. Avetisyan, Yu. M. Goryachev, et al.; *UKRAINSKIY FIZICHESKIY ZHURNAL* Vol 36 No 5, May 91] 3
- Defect Formation Processes and Their Effect on Mechanical Strain in Green Luminescence Gallium Phosphide Structures
 [N. D. Vasilenko, V. A. Krasnov, et al.; *IZVESTIYA VYSSHIKH UCHEBNYKH ZAVEDENIY: FIZIKA* Vol 34 No 1, Jan 91] 3
- Magnetic Exciton Cooling in GaAs
 [Yu. V. Zhilyayev, V. V. Rossin, et al.; *ZHURNAL EKSPERIMENTALNOY I TEORETICHESKOY FIZIKI* Vol 99 No 4, Apr 91] 3

Lasers

- Effect of External Electric Field on Polystyrene's Laser Breakdown
 [N. P. Voloshin, V. A. Vorobey, et al.; *PISMA V ZHURNAL TEKHNIЧЕСКОY FIZIKI* Vol 47 No 4, Feb 91] 5
- On Theory of Relativistic Parametric Electron Wave Free Electron Lasers
 [V. V. Kulish; *UKRAINSKIY FIZICHESKIY ZHURNAL* Vol 36 No 5, May 91] 5
- Resonance Laser-Induced Breakdown on Metal Surface
 [D. V. Gaydarenko, A. G. Leonov; *PISMA V ZHURNAL EKSPERIMENTALNOY I TEORETICHESKOY FIZIKI* Vol 53 No 6, 25 Mar 91] 5
- CO₂-Laser With Fast Frequency Tuning and Stabilization
 [I. M. Belousova, A. S. Grenishin, et al.; *IZVESTIYA AKADEMII NAUK SSSR: SERIYA FIZICHESKAYA* Vol 55 No 2, Feb 91] 6
- Electrooptic Continuous-Duty Deflectors of High-Intensity Laser Radiation
 [A. B. Vankov, V. M. Volynkin, et al.; *IZVESTIYA AKADEMII NAUK SSSR: SERIYA FIZICHESKAYA* Vol 55 No 2, Feb 91] 6
- Energy of Subpicosecond Excimer-Laser Pulse Amplification Saturation
 [V. T. Platonenko, M. K. Shayakhmetova; *IZVESTIYA AKADEMII NAUK SSSR: SERIYA FIZICHESKAYA* Vol 55 No 2, Feb 91] 7

Compression and Stabilization of Ultrashort Laser Pulses in Periodically Nonhomogeneous Optical Fiber [V. A. Vysloukh, L. P. Gevorkyan; <i>IZVESTIYA AKADEMII NAUK SSSR: SERIYA FIZICHESKAYA</i> Vol 55 No 2, Feb 91]	7
Generation of Picosecond X-Ray Pulses in Dense Plasma Produced by High-Intensity Femtosecond Laser Pulses of 308 nm Radiation [S. A. Akhmanov, I. M. Bayanov, et al.; <i>KVANTOVAYA ELEKTRONIKA</i> Vol 18 No 3, Mar 91]	8
Neodymium-Glass Laser With Two Emission Channels and Continuous Regulation of Time Difference and Tunable Time Delay Between Them [N. S. Vorobyev, O. A. Konoplev; <i>KVANTOVAYA ELEKTRONIKA</i> Vol 18 No 3, Mar 91]	8
Two-Stage Shortening of XeCl-Laser Pulse by Stimulated Mandelshtam-Brillouin Scattering [M. S. Dzhidzhoyev, S. V. Krayushkin, et al.; <i>KVANTOVAYA ELEKTRONIKA</i> Vol 18 No 3, Mar 91]	9
Accounting for Field Distribution in Optical Cavity When Determining Optimum Transmittance of Exit Mirror [V. A. Malyshev; <i>KVANTOVAYA ELEKTRONIKA</i> Vol 18 No 3, Mar 91]	9
Lanthanum Scandoborate: New Highly Efficient Solid State Laser Medium [S. A. Kutovoy, V. V. Laptev, et al.; <i>KVANTOVAYA ELEKTRONIKA</i> Vol 18 No 2, Feb 91]	10
Repetitively Pulsed 600 W XeCl Industrial Laser [V. M. Borisov, A. Yu. Vinokhodov, et al.; <i>KVANTOVAYA ELEKTRONIKA</i> Vol 18 No 2, Feb 91]	10
On Ultimate Duration of Ultrashort Light Pulses Emitted by Passive Mode-Locked Solid State Lasers [K. P. Komarov, A. S. Kuchyanov; <i>KVANTOVAYA ELEKTRONIKA</i> Vol 18 No 2, Feb 91]	10
Laser Plasma Flow Collision With Annular Obstacle and Autoionization Ion State Excitation in Oblique Shock Waves [V. A. Boyko, N. P. Datskevich, et al.; <i>KVANTOVAYA ELEKTRONIKA</i> Vol 18 No 2, Feb 91]	11
Origins of Cornea and Skin Ablation by Infrared Laser Irradiation [N. P. Furzikov; <i>KVANTOVAYA ELEKTRONIKA</i> Vol 18 No 2, Feb 91]	11
Periodically Pulsed Composite Discharge-Pumped Diffusion-Cooled CO ₂ Laser [A. F. Vitshas, A. N. Kushko, et al.; <i>PISMA V ZHURNAL TEKHNIЧЕСКОY FIZIKI</i> Vol 17 No 10, May 91]	11

Molecular Physics

Origin of Aromagnetism [M. A. Martsenyuk, N. M. Martsenyuk; <i>PISMA V ZHURNAL EKSPERIMENTALNOY I TEORETICHESKOY FIZIKI</i> Vol 53 No 5, 10 Mar 91]	12
--	----

Nuclear Physics

Excited Muonium Atom State in Condensed Nitrogen [V. G. Grebennik, V. N. Duginov, et al.; <i>FIZIKA NIZKIKH TEMPERATUR</i> Vol 17 No 1, Jan 91]	13
Cold Uranium Fragmentation by Thermal and Fast Neutrons [V. A. Khryachkov, A. A. Goverdovskiy, et al.; <i>YADERNAYA FIZIKA</i> Vol 53 No 3, Mar 91]	13
Iterated Potential Method. Realistic NN-Potential [A. M. Gorbato, V. L. Skopich, et al.; <i>YADERNAYA FIZIKA</i> Vol 53 No 3, Mar 91]	13
Study of Leading s-Quark Hadronization During Inclusive K ⁰ (892)- and K ⁰ -Meson Production on Nuclei [Yu. A. Kulchitskiy; <i>YADERNAYA FIZIKA</i> Vol 53 No 3, Mar 91]	14
Superstring Z'-Boson and t-Quark Mass [V. A. Bednyakov; <i>YADERNAYA FIZIKA</i> Vol 53 No 3, Mar 91]	14
Crystal Structure and Morphology of Epitaxial Germanium Sillenite Layers Deposited by Reactive Cathode Sputtering [A. N. Ognev, V. N. Kornetov, et al.; <i>KRISTALLOGRAFIYA</i> , Vol 36 No 2, Mar 91]	14
Yield of Heavy Quarks in High-Energy Processes [Ye. M. Levin, M. G. Ryskin, et al.; <i>PISMA V ZHURNAL EKSPERIMENTALNOY I TEORETICHESKOY FIZIKI</i> Vol 53 No 6, 25 Mar 91]	14
Mechanism of Steel Hardening by Cyclic Treatment With Low-Energy High-Current Electron Beam [V. I. Itin, I. S. Kashinskaya, et al.; <i>PISMA V ZHURNAL TEKHNIЧЕСКОY FIZIKI</i> Vol 17 No 5, 12 Mar 91]	15
New Kind of Nonexchange Surface Spin Waves in Planar Ferrite-Dielectric-Ferrite Structure [S. V. Tarasenko; <i>PISMA V ZHURNAL TEKHNIЧЕСКОY FIZIKI</i> Vol 17 No 6, 26 Mar 91]	15
New Efficient Isotope Separation Method [B. S. Akshanov, N. A. Khizhnyak; <i>PISMA V ZHURNAL TEKHNIЧЕСКОY FIZIKI</i> Vol 17 No 6, Mar 91]	16

Slab Projection by Explosion [V. I. Bogdanov, A. V. Zvyagin; VESTNIK MOSKOVSKOGO UNIVERSITETA: MATEMATIKA, MEKHANIKA Vol 1 No 2, Mar-Apr 91]	16
High-Power Soft X-Ray Flux Generation in 'Angara-5-1' Unit [V. D. Vikharev, S. V. Zakharov, et al.; ZHURNAL EKSPERIMENTALNOY I TEORETICHESKOY FIZIKI Vol 99 No 4, Apr 91]	16
Photoexcited Electron Momentum Alignment and Spin Orientation in Quantum Wells [I. A. Merkulov, V. I. Perel, et al.; ZHURNAL EKSPERIMENTALNOY I TEORETICHESKOY FIZIKI Vol 99 No 4, Apr 91]	17
Neutron Resonance Examination and Search For Unusual Excited States [G. V. Muradian; YADERNAYA FIZIKA Vol 53 No 4, Apr 91]	17
Search For Prompt Neutrino Production in pA-Interaction at 70 GeV Energies Using SCAT Bubble Chamber [V. V. Ammosov, S. V. Belikov, et al.; YADERNAYA FIZIKA Vol 53 No 4, Apr 91]	17
Search for t-Quarks in Multijet Events at UNK Collider Energies [S. R. Slabospitskiy, M. V. Shevlyagin; YADERNAYA FIZIKA Vol 53 No 4, Apr 91]	17

Optics, Spectroscopy

Is Fundamental Schroedinger Soliton Stabilized in Its Own Nonlinear Optical Fiber? [A. V. Belinskiy; ZHURNAL EKSPERIMENTALNOY I TEORETICHESKOY FIZIKI Vol 99 No 3, Mar 91]	19
Passive Fiber Optic Magnetic Field Transducer With Frequency Output [A. N. Zalogin, S. M. Kozel, et al.; PISMA V ZHURNAL TEKHNIЧЕСКОY FIZIKI Vol 47 No 4, Feb 91]	19
On Limit of Resolution of Intracavity Laser Spectroscopy Method Using FM Resonances [M. V. Danilevko, V. N. Nechiporenko, et al.; UKRAINSKIY FIZICHESKIY ZHURNAL Vol 36 No 5, May 91]	19
On Mechanism of New Radiation Type Development During Relativistic Electron Channeling in Crystal [V. G. Bagrov, I. M. Ternov, et al.; IZVESTIYA VYSSHIKH UCHEBNYKH ZAVEDENIY: FIZIKA Vol 34 No 1, Jan 91]	20
Spatial Polarization Solitons in Vector Theory of Self-Focusing [F. N. Marchevskiy, V. L. Strizhevskiy, et al.; IZVESTIYA AKADEMII NAUK: SERIYA FIZICHESKAYA Vol 55 No 2, Feb 91]	20
Evolution of Quantum Fluctuations During Nonlinear Propagation of Fundamental Soliton [A. V. Belinskiy; IZVESTIYA AKADEMII NAUK SSSR: SERIYA FIZICHESKAYA Vol 55 No 2, Feb 91]	20
Fiber-Optic Magnetic Field Strength Microscope [S. M. Kozel, V. N. Listvin, et al.; PISMA V ZHURNAL TEKHNIЧЕСКОY FIZIKI Vol 17 No 5, 12 Mar 91]	21
Source of Picosecond Pulses From Semiconductor Laser in Fiber Optical Cavity [I. A. Knyazev, A. S. Shcherbakov, et al.; PISMA V ZHURNAL TEKHNIЧЕСКОY FIZIKI Vol 17 No 3, 12 Feb 91]	21
On Possibility of Synthesizing Three-Dimensional Images Using Gaseous Discharge Light Sources [Yu. B. Golubovskiy, I. E. Suleymenov; PISMA V ZHURNAL TEKHNIЧЕСКОY FIZIKI Vol 17 No 8, Apr 91]	21
Passage of Femtosecond Solitons Through Fiber-Optic Loop [E. A. Zakhidov, F. M. Mirtadzhiev, et al.; KVANTOVAYA ELEKTRONIKA Vol 18 No 3, Mar 91]	22
Effect of Aging on X-Ray Optics of Ta/Al Multilayer Interference Structures [A. G. Lyubimov, Yuen Kshyan-Yang, et al.; PISMA V ZHURNAL TEKHNIЧЕСКОY FIZIKI Vol 17 No 6, 26 Mar 91]	22
Fractal Dynamics of Deformable Media [A. S. Balankin; PISMA V ZHURNAL TEKHNIЧЕСКОY FIZIKI Vol 17 No 6, 26 Mar 91]	22
Stimulated Diffuse Nanosecond Pulse Backscattering in Cumulative Exposure Mode [I. V. Gusev, B. Ya. Zeldovich, et al.; ZHURNAL EKSPERIMENTALNOY I TEORETICHESKOY FIZIKI Vol 99 No 4, Apr 91]	23
Vector Envelope Soliton Bifurcation and Hamiltonian System Integrability [V. M. Yeleonskiy, V. G. Korolev, et al.; ZHURNAL EKSPERIMENTALNOY I TEORETICHESKOY FIZIKI Vol 99 No 4, Apr 91]	23

Nonclassical Bichromatic Field-Induced Optical Effects [G. Yu. Kryuchyan; ZHURNAL EKSPERIMENTALNOY I TEORETICHESKOY FIZIKI Vol 99 No 5, May 91]	24
Charge Density Wave Dislocations in Crystals [S. A. Brazovskiy, S. I. Matveyenko; ZHURNAL EKSPERIMENTALNOY I TEORETICHESKOY FIZIKI Vol 99 No 5, May 91]	24
Three-Wave Interaction in Semiconductors Due to Exciton-Biexciton Mechanism: Additional Boundary Value Condition Problem and Three-Frequency Solitons [A. L. Ivanov, V. V. Panashchenko; ZHURNAL EKSPERIMENTALNOY I TEORETICHESKOY FIZIKI Vol 99 No 5, May 91]	24
Optically Controlled VO ₂ Film-Based Fiber Switch [F. A. Yegorov, Yu. Sh. Temirov, et al.; PISMA V ZHURNAL TEKHNIЧЕСКОY FIZIKI Vol 17 No 9, May 91]	25

Plasma Physics

Plasma in Intense Sound Wave Field [A. R. Aramyan, G. A. Galechyan, et al.; AKUSTICHESKIY ZHURNAL Vol 37 No 2, Mar-Apr 91]	26
On Some Relaxation Behavior Anomalies of Supercooled Liquids Based on Acoustic Experiment Data [A. A. Berdyyev, A. V. Rudin, et al.; AKUSTICHESKIY ZHURNAL Vol 37 No 2, Mar-Apr 91]	26
Using New Approaches to Compute Scalar Wave Field's Scattering Coefficient of Statistically Rough Surface With Complex Spectral Composition [M. Yu. Galaktionov; AKUSTICHESKIY ZHURNAL Vol 37 No 2, Mar-Apr 91]	26
New Material for Acoustic Converters [O. A. Kapustina; AKUSTICHESKIY ZHURNAL Vol 37 No 2, Mar-Apr 91]	26
Nonlinear m = 1 Flute Mode Stability in Nonparaxial Open Confinement System [I. M. Lanskiy, G. V. Stupakov; FIZIKA PLAZMY Vol 17 No 3, Mar 91]	27
High-Frequency Surface Potential Waves on Metal's Boundary With Magnetoactive Plasma of Finite Pressure [N. A. Azarenkov, K. N. Ostrikov; FIZIKA PLAZMY Vol 17 No 3, Mar 91]	27
Nonlinear Electromagnetic Energy Emission by Surface Waves From Plasma Films of Variable Thickness [A. A. Zharov, A. I. Smirnov; FIZIKA PLAZMY Vol 17 No 3, Mar 91]	27
Investigation of Intense Electromagnetic Pulse Transit Through Vacuum Line With Plasma Jumper [L. Ye. Aranchuk, V. M. Babykin, et al.; FIZIKA PLAZMY Vol 17 No 5, Apr 91]	28
Particle Acceleration Under Effect of RF Field on Expanding Plasma [S. V. Bulanov, I. N. Inovenkov, et al.; FIZIKA PLAZMY Vol 17 No 5, Apr 91]	28
Experimental Study of Beam-Plasma Instability of Long-Pulse Monoenergetic Relativistic Electron Beam in Gas [V. M. Batenin, V. S. Zhivopistsev, et al.; FIZIKA PLAZMY Vol 17 No 4, Apr 91]	28
Intense Relativistic Electron Beam Propagation in Low-Density Plasma [V. B. Krasovitskiy, O. Yu. Naguchev, et al.; FIZIKA PLAZMY Vol 17 No 4, Apr 91]	29

Superconductivity

Elevation of Thin-Film Superconducting Transition Temperature Due to Deposition of Normal Metal on Surface [I. L. Landau, D. L. Shapovalov, et al.; PISMA V ZHURNAL EKSPERIMENTALNOY I TEORETICHESKOY FIZIKI Vol 53 No 5, 10 Mar 91]	30
Elasticity, Strength, and Fracture Character of High-T _c YBa ₂ Cu ₃ O _{7-δ} Ceramics of Varying Density in 4.2-293K Temperature Range [V. N. Kovaleva, V. A. Moskalenko, et al.; FIZIKA NIZKIKH TEMPERATUR Vol 17 No 1, Jan 91]	30
Temperature Anomalies of Yttrium Ceramics Impedance and Heat Capacity at T ≥ T _c [V. M. Dmitriyev, V. N. Yeropkin, et al.; FIZIKA NIZKIKH TEMPERATUR Vol 17 No 1, Jan 91]	30
Superconductivity Destruction by Optical Radiation in Nonequilibrium Resistive States and YBa ₂ Cu ₃ O _{7-x} High-T _c Films [P. P. Vysheslavtsev, G. M. Genkin, et al.; ZHURNAL EKSPERIMENTALNOY I TEORETICHESKOY FIZIKI Vol 99 No 3, Mar 91]	31
Josephson Junction With Ferromagnetic Interlayer [A. I. Buzdin, M. Yu. Kupriyanov; PISMA V ZHURNAL EKSPERIMENTALNOY I TEORETICHESKOY FIZIKI Vol 53 No 6, 25 Mar 91]	31
Theory of Superconducting SF and SFS Structures in Pure Limit at Temperatures Far Below Critical [S. V. Kuplevakhskiy, I. I. Falko; TEORETICHESKAYA I MATEMATICHESKAYA FIZIKA Vol 86 No 2, Feb 91]	31

Superconductivity in System of Electrons With Four-Fermion Tunneling Hamiltonian [M. Ye. Zhuravlev, V. A. Ivanov; <i>TEORETICHESKAYA I MATEMATICHESKAYA FIZIKA</i> Vol 86 No 2, Feb 91]	32
Production of Thin Ti-Ba-Ca-Cu-O High- T_c Superconductor Films [O. R. Baydakov, V. N. Golubev, et al.; <i>PISMA V ZHURNAL TEKHNIЧЕСКОY FIZIKI</i> Vol 17 No 6, 26 Mar 91]	32
Bisoliton Model of High- T_c Superconductivity: Review [A. S. Davydov; <i>UKRAINSKIY FIZICHESKIY ZHURNAL</i> Vol 36 No 3, Mar 91]	33
On New Class of Normal Fermi-Fluids [G. Ye. Volovik; <i>PISMA V ZHURNAL EKSPERIMENTALNOY I TEORETICHESKOY FIZIKI</i> Vol 53 No 4, Feb 91]	33
Magnetization Characteristics of Highly Anisotropic Superconductors [N. V. Zavaritskiy, V. N. Zavaritskiy; <i>PISMA V ZHURNAL EKSPERIMENTALNOY I TEORETICHESKOY FIZIKI</i> Vol 53 No 4, Feb 91]	33
Electron-Induced Light Scattering in Conducting High- T_c State [V. N. Kostur, G. M. Eliashberg; <i>PISMA V ZHURNAL EKSPERIMENTALNOY I TEORETICHESKOY FIZIKI</i> Vol 53 No 7, Apr 91]	34
On Temperature Dependence of Field Penetration Depth in Superconductors [G. V. Klimovich, A. V. Rylyakov, et al.; <i>PISMA V ZHURNAL EKSPERIMENTALNOY I TEORETICHESKOY FIZIKI</i> Vol 53 No 7, Apr 91]	34
Dependence of Bi-Sr-Ca-Cu-O:Pb Gap Parameter on Temperature [L. I. Leonyuk, M. V. Pedyash, et al.; <i>PISMA V ZHURNAL TEKHNIЧЕСКОY FIZIKI</i> Vol 17 No 9, May 91]	34
On Physical Origin of Superconducting Polar Elastomer Channels [L. N. Grigorov; <i>PISMA V ZHURNAL TEKHNIЧЕСКОY FIZIKI</i> Vol 17 No 10, May 91]	34
Effect of $YBa_2Cu_3O_{7.8}$ Superconducting Metal Oxide Doping With Boron Nitride on its Properties [Ye. M. Gololobov, I. I. Papp, et al.; <i>PISMA V ZHURNAL TEKHNIЧЕСКОY FIZIKI</i> Vol 17 No 8, Apr 91]	35

Technical Physics

On New Trend in Microelectronic Magnetic Storage Device Technology [A. N. Averkin, V. P. Dmitriyev; <i>PISMA V ZHURNAL TEKHNIЧЕСКОY FIZIKI</i> Vol 17 No 9, May 91]	36
--	----

Theoretical Physics

New Approach to Problem of Detecting Gravitational Waves [A. B. Balakin, G. V. Kisunko, et al.; <i>PISMA V ZHURNAL EKSPERIMENTALNOY I TEORETICHESKOY FIZIKI</i> Vol 53 No 6, 25 Mar 91]	37
--	----

Nonlinear Dynamics and Abnormal Electroacoustic Wave Attenuation in Order-Disorder Ferroelectrics

917J0091B Moscow *ZHURNAL EKSPERIMENTALNOY I TEORETICHESKOY FIZIKI in Russian* Vol 99 No 3, Mar 91 pp 860-873

[Article by M. B. Belonenko, M. M. Shakirzyanov, Kazan Engineering Physics Institute imeni Ye. K. Zavoyskiy at the Kazan Branch of the USSR Academy of Sciences]

[Abstract] Effects of electroacoustic (EA) echo in single crystals of KDP and Rs ferroelectrics which display an abnormal behavior of the EA wave attenuation near the order-disorder phase transition point are discussed. In the authors' opinion, all significant dynamic characteristics of ferroelectric crystals excited by alternating electric fields may be described with the help of the pseudospin (PS) formalism widely used in the ferroelectric theory. A theory of electric echo in KDP ferroelectrics characterized by a symmetric double-well potential for protons in the hydrogen bond is developed on the basis of a pseudospin formalism. This system's Hamiltonian in the pseudospin formalism assumes the form of Ising's Hamiltonian in intersecting fields. A set of effective differential equations for envelopes of forward and backward electroacoustic wave is found; an expression for effective electroacoustic wave damping factor is derived from these equations. This damping factor's dependence on temperature is consistent with the experimental relation. An expression for the amplitude of the electroacoustic echo resulting from the parametric interaction of the forward electroacoustic wave and a uniform electric field of the second pulse is obtained and the linear dependence of the echo amplitude on the alternating field amplitude and pulse duration if the ferroelectric is excited by low-intensity pulses is explained. The absence of echo in the ferroelectric paraphase at a null electric field and a strong echo signal attenuation when the samples are deuterated are explained. It is shown that the resulting theory correctly describes available experimental data and makes it possible to calculate the characteristics of electroacoustic echo on the basis of microscopic notions of ferroelectricity. The authors are grateful to A. R. Kessel for formulating the problem and giving advice and to V. M. Berezov and V. G. Bakurov for useful discussion. References 15: 12 Russian; 3 Western.

Speed of Sound in He-CO₂ Mixtures Under High Pressures

917J0101A Moscow *DOKLADY AKADEMII NAUK SSSR in Russian* Vol 316 No 5, Feb 91 pp 1112-1116

[Article by L. L. Pitayevskaya and A. A. Popov, Institute of High-Temperature Physics imeni L. F. Vereshchagin, USSR Academy of Sciences, Troitsk (Moscow Oblast)]

UDC 534.614:533.27

[Abstract] An experimental study of the He-CO₂ system under rising pressure was made for the purpose of acoustically detecting the separation of the two gases from their homogeneous mixture and thus determining the pressure dependence of the He-solubility limit in CO₂ on the basis of the speed of sound, that limit being known to drop to lower He mol.% concentrations under rising pressure and gas-gas equilibrium being known to prevail at temperatures above the critical point for the less volatile CO₂ (305.25 K, liquid-gas equilibrium below that point). The speed of sound in mixtures with 22.9, 42.1, 50.6, 58.3, 69.9, and 82.1 mol.% He was measured at temperatures 293.15-308.15 K, 313.5 K, 353.15 K, and 383.15 K under pressures covering the 10-550 MPa range. It was measured by the pulse method with a radiator-receiver pair of 5 MHz X-cut piezoelectric quartz transducers 7 mm apart and a frequency meter operating as a time interval meter, this method involving measurement of the time taken by a sound pulse to travel across the fixed 7 mm distance from radiator to receiver, or by the pulse echo method using two time markers on the screen of an oscillograph. The data, consistent with the He-CO₂ constitution diagram, describe in quantitative form the pressure-concentration (mol.% He) dependence of the speed of sound and thus the pressure dependence of the He solubility limit in CO₂ at those temperatures. Figures 4; tables 2; references 6.

Cumulation Effect During Interaction of Standing Shock Wave and Conical Body

917J0105B Leningrad *PISMA V ZHURNAL TEKHNIЧЕСКОY FIZIKI in Russian* Vol 17 No 5, 12 Mar 91 pp 65-68

[Article by Yu. M. Beletskiy, D. F. Bykov, P. A. Voynovich, Ye. L. Satunina, I. V. Sokolov, and V. Ye. Terekhin]

[Abstract] Interaction of a converging axisymmetric two-dimensional shock wave and the conical tip of a body in a steady supersonic gas stream is analyzed, taking into account the attendant buildup of the shock wave due to the cumulation effect, assuming that the gas is a homogeneous one. The resulting flow pattern is most distinctly characteristic of such an interaction when both the apex half-angle θ_0 of the cone and the angle of attack ν are very small, a $\nu \leq 1$ corresponding to a radial velocity of the shock front being much smaller than the axial velocity of the gas stream so that the piston analogy is valid and reflection of a cylindrical shock wave by an acute cone corresponds to its reflection by an expanding cylindrical piston. The analysis is accordingly based on a system of two first-order partial differential equations describing radial flow upon incidence of a cylindrical shock wave in the $O(\theta_0^2) + O(\nu^2)$ approximation. The results are compared with a shadowgram which depicts reflection of a converging cylindrical shock wave by a conical tip, a conical tip with a 20° apex half-angle having been placed in a jet discharging from a De Laval

nozzle at a velocity of $N_{Ma} \approx 3$ under a static pressure of 140 torr into a stream under a static pressure of about 200 torr. The cumulation effect was simulated numerically on a uniform Lagrangian checkerboard grid of 200 cells. The results indicate the possibility of a gas density and pressure increase by a large factor during interaction of such a standing shock wave and a conical tip. Figures 3; references 13.

Shock Waves in Developing Gas Discharge

917J0106B Leningrad PISMA V ZHURNAL
TEKHNICHESKOY FIZIKI in Russian Vol 17 No 3,
12 Feb 91 pp 59-62

[Article by Yu. I. Chutov, V. N. Podolskiy, and D. A. Brayon]

[Abstract] An experimental study of shock waves generated by short discharge pulses in a nitrogen or argon plasma was made, an electric shock tube made of glass and 2 cm in diameter having been filled with gas to a pressure of 1 torr and the two electrodes having been connected to a capacitor bank discharging through a resistor. The time constant of the discharge circuit was $RC = 0.5$ s, but quasi-steady discharge was limited to a pulse of about 100 μ s duration. Such a discharge generated 20-30 cm long shock waves in the tube, with the initial discharge current density not exceeding 0.7 A/cm². The velocity of such shock waves was measured at various distances from the center of the tube, where the anode was located and discharge originated, at successive instants of time after the beginning of discharge. As a function of time, in the nitrogen plasma their velocity first increased to a maximum after 2 ms and then stabilized at a lower level after 4 ms. In the argon plasma their velocity increased monotonically to a stable level. In the nitrogen plasma both their maximum and steady-state velocities were highest at approximately 5 cm from the center, while in neutral nitrogen their velocity

decreased monotonically with increasing distance from the center. The ratio V_m/V_0 of the maximum velocity in ionized nitrogen to the velocity in neutral nitrogen was found to increase linearly with increasing distance from the center, while the ratio V_{ss}/V_0 of the steady-state velocity in ionized nitrogen or argon to the velocity in the respective neutral gas was found to remain almost the same with increasing distance from the center. These trends indicate the extent to which compression of the gas, and its rarefaction by heating, influence the attenuation of such shock waves in these media. Figures 2; references 17.

Relativistic Electron Beam Propagation in Extragalactic Jet Plasma in Gas Dynamic Approximation

917J0116A Kiev UKRAINSKIY FIZICHESKIY
ZHURNAL in Ukrainian Vol 36 No 3, Mar 91
pp 364-369

[Article by V. M. Melnik, Radioastronomy Institute at the Ukrainian Academy of Sciences, Kharkov]

UDC 533.9

[Abstract] One-dimensional propagation of a beam of relativistic electrons through the plasma of extragalactic jets where the time of quasilinear relaxation is short compared to the electron dissociation time is considered. A closed system of gas dynamic equations is derived for fast electrons and plasmons generated by them. A self-similar solution of this system of equations which represents a beam-plasma formation traveling at a constant velocity v_m , c , where c is the speed of light, and a constant Γ -factor $\Gamma_m \approx$ square root of $\Gamma/2$, where $\Gamma \gg 1$ for the fastest beam-plasma formation electrons, is found. The author is grateful to J. Roland for making available the results of his study before publication. Figures 4; references 8: 3 Russian, 5 Western.

Solitons in Charge Density Wave Crystals

917J0091C Moscow *ZHURNAL
EKSPERIMENTALNOY I TEORETICHESKOY
FIZIKI* in Russian Vol 99 No 3, Mar 91 pp 887-897

[Article by S. A. Brazovskiy, S. I. Matveyenko, Theoretical Physics Institute imeni L. D. Landau at the USSR Academy of Sciences]

[Abstract] Electronic properties of quasiunidimensional conductors with a charge density wave (VZP) are summarized. Effects of long-range structural deformations and Coulomb fields appearing during the CDW crystalline medium adaptation to various solitons generated in the course of electron conversion are examined. Static deformations in a three-dimensional ordered CDW medium with point solitons and soliton interactions with each other and impurities are analyzed. Screening by extrinsic carriers and self-screening in a soliton gas are considered. A model is developed for describing the soliton structure in ordered crystalline media. A model-independent approach is suggested for describing the interaction of solitons with long-range Coulomb and deformation fields; in addition, combined effects of weak commensurability are examined. Soliton attraction domains are found for all areas. The results of the study make it possible to outline a microscopic pattern of successive stages of normal current conversion to Froehlich's CDW slip current. They also show a trend toward aggregation of solitons into complexes equivalent to dislocation loops. Figures 1; references 20: 3 Russian, 17 Western.

Electrophysical Properties of $\text{HfNi}_{1-x}\text{Co}_x\text{Sn}$ ($0 \leq x \leq 0.4$) Compounds

917J0095C Kiev *UKRAINSKIY FIZICHESKIY
ZHURNAL* in Russian Vol 36 No 5, May 91
pp 773-775

[Article by A. O. Avetisyan, Yu. M. Goryachev, S. V. Kalchenko, R. V. Skolozdra, Yu. V. Stadnyk, Institute of Materials Science Problems at the Ukrainian Academy of Sciences, Kiev and Lvov University imeni Iv. Franko]

UDC 539.192

[Abstract] $\text{HfNi}_{1-x}\text{Co}_x\text{Sn}$ ($0 \leq x \leq 0.4$) compounds' electrophysical properties are examined for the first time in the 300-1,300K temperature range. The ternary HfNiSn compound has a MgAgAs -type structure characterized by a vacancy lattice (relative to nickel). Polycrystalline $\text{HfNi}_{1-x}\text{Co}_x\text{Sn}$ ($0 \leq x \leq 0.4$) samples were obtained by melting a mixture of at least 99.99 percent pure initial components in an electric arc furnace in an atmosphere of purified argon. The results of the study show that the compounds display semiconductor properties within said temperature range; as the temperature rises, the resistivity decreases. A substitution of nickel with cobalt in the HfNiSn compound leads to a change in the sign of the $\text{HfNi}_{1-x}\text{Co}_x\text{Sn}$ ($0 \leq x \leq 0.4$) compound's thermo-EMF

from negative to positive. Such peculiarities of these compounds' electrophysical properties are probably due to a combination of characteristic features of their crystal structure and electronic arrangement. Figures 2; references 5.

Defect Formation Processes and Their Effect on Mechanical Strain in Green Luminescence Gallium Phosphide Structures

917J0096A Tomsk *IZVESTIYA VYSSHIKH
UCHEBNIKH ZAVEDENIY: FIZIKA* in Russian
Vol 34 No 1, Jan 91 pp 23-27

[Article by N. D. Vasilenko, V. A. Krasnov, A. N. Kryzhanovskiy, V. M. Cherner, Odessa State University imeni I. I. Mechnikov]

UDC 548.4-143

[Abstract] Defect formation and its effect on internal mechanical strain (VMN) in gallium phosphide layers doped with nitrogen and containing gallium nitride inclusions is investigated; to this end, generation of defects and their effect on internal mechanical strain in epitaxial GaP layers grown from a GaP melt by adding finely dispersed (0.1-0.3 μm) GaN particles in an atmosphere of nitrogen with ammonia is examined. In addition, the layers were doped with nitrogen by blasting a gaseous hydrogen and ammonia mixture over the molten solution during the epitaxy process. It is established that an increase in the ammonia content in the mixture from 0.04 to 0.1 percent by volume leads to an increase in the number of defects, particularly the inclusions of second phase, as well as internal strain, while an increase in the ammonia content to more than 0.1 percent—to the development of small cracks and stress relaxation. The dependence of internal mechanical strain on GaN volumetric fraction and degree of dispersion in GaP is established. A mathematical model of the processes is developed and the results are discussed in the framework of this model. It is shown that theoretical results are consistent with experimental data. Figures 2; references 9.

Magnetic Exciton Cooling in GaAs

917J0119E Moscow *ZHURNAL
EKSPERIMENTALNOY I TEORETICHESKOY
FIZIKI* in Russian Vol 99 No 4, Apr 91 pp 1241-1253

[Article by Yu. V. Zhilyayev, V. V. Rossin, T. V. Rossina, V. V. Travnikov, Engineering Physics Institute imeni A. F. Ioffe at the USSR Academy of Sciences]

[Abstract] The effect of magnetic field on the energy structure of excitons, particularly the diamagnetic shift and Zeeman's splitting of fundamental and excited states, and polariton luminescence (PL) enhancement in GaAs in a magnetic field examined by other researchers is summarized. The results of a detailed investigation of the latter phenomenon which is directly attributed to the

effect of magnetic field on exciton kinetic are presented and manifestations of this phenomenon observed experimentally are described. An analysis of abnormal polariton luminescent enhancement in superpure epitaxial GaAs layers in a magnetic field of up to 7 T shows that this enhancement is due to the fact that excitons are effectively cooled in the magnetic field almost to the lattice temperature. It is speculated that a decrease in the effective exciton temperature in the magnetic field is caused by an increase in the rate of electron energy relaxation and electron cooling. The electron energy

relaxation in the magnetic field is computed analytically. A mechanism of polariton luminescence enhancement is proposed and discussed and it is shown that the polariton energy distribution function is largely determined by exciton-electron scattering processes. In the magnetic field strength range under study, the effective nonequilibrium electron temperature drops sharply due to an increase in the energy relaxation rate in acoustic phonons. The authors are grateful to V. A. Kharchenko for fruitful discussions which facilitated this effort. Figures 8; references 22: 15 Russian, 7 Western.

Effect of External Electric Field on Polystyrene's Laser Breakdown

917J0094B Leningrad PISMA V ZHURNAL
TEKHNICHESKOY FIZIKI in Russian Vol 47 No 4,
Feb 91 pp 89-92

[Article by N. P. Voloshin, V. A. Vorobey, A. V. Znamenskiy, A. T. Chistyakov, All-Union Scientific Research Institute of Engineering Physics, Chelyabinsk]

[Abstract] The development of shear defects in the maximum tangential stress plane of transparent organic materials irradiated by lasers which are manifested as disc-shaped cracks oriented at about 45° to the laser beam due to of the wedging pressure exerted by the gas produced by the dissipation of light energy in absorbing centers is discussed. The results of preliminary experiments to examine the effect of external electric field on laser-induced polystyrene breakdown are cited. The samples were placed in a static external electric field and irradiated by laser in two ways: parallel and perpendicular to the electric field's lines of force. A free running neodymium laser at a $\lambda = 1.06 \mu\text{m}$ wavelength emitting $1 \mu\text{s}$ pulses with an energy density of 5 MW/cm^2 injected into the samples without focusing elements was used; the beam had a 6 mm diameter and a $\leq 10^\circ$ divergence. Cylindrical 50 mm long samples with a 70 mm diameter were used. The study demonstrates that an external electric field changes the effect of high-power laser radiation on polymers. It is noted that additional experiments are necessary to draw more specific conclusions. The samples used in the aforesaid experiments were checked for the presence of synthetic diamond in the cracks; none was found. The authors are grateful to L. I. Karpovitskaya and I. V. Podgornova for help with the experiments, A. S. Vladimirov to valuable discussions, and N. P. Kozeruk for looking for synthetic diamond in chemical decomposition products. Figures 2; references 6.

On Theory of Relativistic Parametric Electron Wave Free Electron Lasers

917J0095B Kiev UKRAINSKIY FIZICHESKIY
ZHURNAL in Russian Vol 36 No 5, May 91
pp 686-693

[Article by V. V. Kulish, Sumy Physical Technology Institute]

UDC 537.86+621.373

[Abstract] The ongoing "reevaluation of concepts" of classical physical electronics due to the emergence of such devices as free electron lasers (LSE) and successful experiments with relativistic electron beams (REP) is addressed and the capabilities of "old" microwave (SVCh) principles being reexamined in the framework of the relativism concept are summarized. A theoretical model is proposed and a weak-signal theory of Raman two-stream free electron laser is developed. The electron stream's fast space charge wave (VPZ) is used as the

working wave; as a result, the conclusion is drawn about potentially low intrinsic noise levels in the laser. The model under study is characterized in that the working fast wave is parametrically bound to two other SCW's one of which serves as an additional electron-wave pump and the other, as an idle signal. Expressions for working frequencies and gain of the signals TEM-wave are derived and analyzed. After comparing their results to typical parameters of free electron lasers, the authors conclude that the issue of developing a low-noise input amplifier for the submillimeter and infrared (IK) bands operating in the CW mode can be practically solved at today's level of technology. The author is grateful to V. Ye. Storizhko for his attention to this study and useful discussions. Figures 1; references 20: 16 Russian, 4 Western.

Resonance Laser-Induced Breakdown on Metal Surface

917J0100B Moscow PISMA V ZHURNAL
EKSPERIMENTALNOY I TEORETICHESKOY
FIZIKI Vol 53 No 6, 25 Mar 91 pp 290-293

[Article by D. V. Gaydarenko and A. G. Leonov, Moscow Institute of Engineering Physics, Dolgoprudnyy]

[Abstract] In an experiment with plasma formation in vapor of a metal upon treatment of the metal surface with a laser beam there was observed, evidently for the first time, a resonance depression of the plasma formation threshold. In this experiment a sodium target was treated with a pulsed LZHI-501 dye laser tunable over the 589.6-589.0 nm range of wavelengths, covering $3^2\text{S}_{1/2} - 3^2\text{P}_{1/2}$ and $3^2\text{S}_{1/2} - 3^2\text{P}_{3/2}$ resonance transitions in the Na atom and pumped with second-harmonic radiation of a YAG:Nd³ solid-state laser. The pulses were of 20 ns wide at half-amplitude level and their energy was varied over the 0-5 mJ range. They were focused on the target within a spot 0.1 mm in diameter, in an interaction chamber under 10^{-4} mm Hg vacuum. Concentration of plasma ions was measured with a plasma probe operating in the saturation mode at a distance of 8-12 cm from the target. The concentration of plasma electrons was measured on the basis of the Stark broadening of both 568.2 nm and 568.8 nm Na-atom lines at a distance of about 0.1 mm with an adjustable time lag behind the beginning of a laser pulse. Probing of the erosion jet included recording glow of the plasma continuum over the 350-400 nm spectral band. On the basis of these measurements, the dependence of the amplitude of the probe signal and the dependence of the amplitude of the continuum glow on the intensity of incident laser radiation were determined. The plasma formation threshold was then estimated in two ways, by extrapolation of each dependence on the laser radiation intensity to zero respective amplitude. The difference between the two estimates of threshold laser radiation intensity did not exceed 20 percent. Such estimates were made for each laser radiation wavelength within the 575-610 nm tuning

range so that the dependence of the threshold laser radiation intensity on the laser radiation wavelength could also be determined. The dependence of the plasma electron concentration on the laser radiation wavelength at constant laser radiation intensity was determined at various levels of that intensity, including 56 MW/cm² and 250 MW/cm². The results reveal a dip of the threshold laser radiation intensity to a low minimum and a peak of the plasma electron concentration to a high maximum extending over the 589.0-589.6 nm wavelength band, which corresponds to resonance 3S-3P transitions in the Na atom, with an up to $\Delta\lambda \approx 8$ nm wide spread of resonance lines attributable to field-effect broadening associated with transition saturation. The authors thank A. N. Starostin for attentiveness and helpful discussion of the results. Figures 3; references 8.

CO₂-Laser With Fast Frequency Tuning and Stabilization

917J0102A Moscow IZVESTIYA AKADEMII NAUK
SSSR: SERIYA FIZICHESKAYA in Russian Vol 55
No 2, Feb 91 pp 227-230

[Article by I. M. Belousova, A. S. Grenishin, N. A. Gryaznov, V. M. Kiselev, and A. V. Pasechnik, State Institute of Optics imeni S. I. Vavilov]

UDC 621.373.826.823

[Abstract] A continuous-wave CO₂-laser with fast frequency stabilization by means of a CdTe electrooptic phase modulator was tested, the modulator being a 34 mm long 10 mm² square bar cut along the (101) axis and the electrooptic field being applied along its (010) axis. The active medium was a CO₂:N₂:He = 1:1:4 mixture under a pressure of 30 torr inside a cell 70 cm long with a 6 mm diameter and Brewster windows. The optical cavity for the active medium and the frequency modulator was formed by a diffraction grating with 150 lines/mm at a 52° blaze angle acting as autocollimator and a plane exit mirror, a ZnSe plate with a reflective dielectric coating ($R = 0.85$). This mirror was mounted on a piezoelectric transducer picking up low-frequency vibrations. The modulator was tested by application of a voltage control pulse of 50 ns duration and with a very short rise time, its amplitude being varied from 700 V to 2700 V. Radiation emitted by the laser and diverted to a KRT-2 photodetector by a slanting semitransparent plane mirror was mixed in that photodetector with radiation from a reference laser, whereupon the resulting beats were boosted by two successive U3-33 amplifiers and then recorded on an S1-75 oscillograph. Calculations based on the experimental data indicate that a modulator sensitivity of 5 Hz/V is attainable with an optimally cut bar of the same dimensions and optimally positioned in the same optical cavity, a sensitivity of 8 kHz/V being feasible with a thinner 6x6 mm² square bar and a still higher sensitivity being feasible with a thicker bar but requiring a smaller absorption coefficient. The laser amplifier bandwidth was so wide, 100-150 MHz,

that the dependence of the emission power on the frequency deviation was weak. It was therefore necessary to simultaneously ensure a large amplitude of the frequency modulation signal and a large amplitude of the only 20 MHz wide frequency deviation signal so as to ensure an adequate sensitivity of the latter. Frequency stabilization was effected at the P(20)-line of the active heterodyne transition, the amplifier of this line being the principal deviation frequency discriminator, while the modulation frequency had to be raised from 1 MHz to 3 MHz for effective suppression of mechanical vibrations of the modulator crystal at resonance. As a result, a frequency stability within 10⁻⁸ was attained with a maximum frequency deviation of 150 kHz necessary for normal operation at a level three times higher than the noise level. Figures 2; references 4.

Electrooptic Continuous-Duty Deflectors of High-Intensity Laser Radiation

917J0102B Moscow IZVESTIYA AKADEMII NAUK
SSSR: SERIYA FIZICHESKAYA in Russian Vol 55
No 2, Feb 91 pp 253-259

[Article by A. B. Vankov, V. M. Volynkin, and A. A. Chertkov, State Institute of Optics imeni S. I. Vavilov]

UDC 621.376

[Abstract] The performance of electrooptic crystals as prismatic radiation deflectors is evaluated both theoretically and on the basis of experimental data, LiNbO₃ and LiTaO₃ as well as DKDP crystals being considered for continuous deflection of high-intensity laser radiation particularly so because they can be cooled to temperatures near the Curie point. A reflection deflector consists of one isosceles right triangular prism with two total internal reflections ($k = 2$) or several successive identical such prisms ($k = 4, 6, \dots$). A transmission deflector is a pair of identical preferably scalene right triangular prisms with their bases contiguous or close and parallel to each other so that they form a diagonally split rectangular cell. The deflection angle is $\beta = kn_0^3 r_{63} E$ for a reflection deflector and $\beta = \tan \beta n_0^3 r_{63} E$ for a transmission deflector (n_0 - refractive index of a crystal for the ordinary ray, r_{63} - electrooptic coefficient, E - intensity of the applied electric field, k - number of total internal reflections. Total internal reflections in a transmission deflector inhibit wide deflection and need to be prevented, which can be done by immersion in a fluid with a refractive index approximately equal to that of the crystals. Inasmuch as the number N of resolvable elements is proportional to the deflection angle β and inversely proportional to the radiation wavelength λ ($N = \beta / 1.2\lambda$), one can optimize a deflector by maximizing the number N of resolvable elements for unipolar control or for bipolar control of a reflection deflector and of a transmission deflector. This has been done for each kind of deflector by determining the aperture necessary for attaining the maximum N , assuming each crystal with an electrooptic coefficient $r_{63} = 8 \times 10^{-8}$ cm/V in an electric

field of $E = 20$ kV/cm intensity to be at a temperature 4-5° above the Curie point (further cooling having been found not to be worthwhile). Inasmuch as the dielectric strength of crystals is finite, bipolar control allows a wider deflection and therefore is preferable. Owing to the piezoelectric effect, control by application of longer than nanosecond voltage pulses gives rise to crystal deformations which will change the deflection angle. Their influence can be compensated by phase conjugation or by back-reflection of the laser beam. Inasmuch as the electrooptic effect causes deflection of the ordinary ray only while the piezoelectric effect causes deflection of both ordinary and extraordinary rays in opposite directions, it is possible to compensate the piezoelectric deflection while retaining the electrooptic deflection. An incident laser beam polarized as is the extraordinary ray is passed from the deflector through a quarter-wave plate to a reflector which consists of a planoconvex lens followed by a concave mirror and sends the laser beam back through that quarter-wave plate to the deflector for a return passage through it. Replacement of such a reflector with a plain plane mirror perpendicular to the path of a nonpolarized laser beam will ensure its compensated deflection. Experiments were performed with two XY-deflectors of $\lambda = 1.06$ μm laser radiation at -70°C, one consisting of two DKDP transmission cells immersed in an organic fluid breaking down electrically under 5 kV/mm with a Love prism between them and one consisting of two successive prisms with two total internal reflections each. Experiments were also performed with quadrupole deflectors of $\lambda = 1.06$ μm laser radiation at room temperature, each consisting of two crystal pairs in quadrature on a square mount and the theoretical deflection angle being $\beta = 4n_0^3 r_{ij} V/D$ (r_{ij} - electrooptic coefficient, V - same voltage applied to both crystal pairs, L - length of deflector, D - diagonal width of deflector assembly). These deflectors were immersed in a fluid with a dielectric strength higher than 5 kV/cm so as to prevent interelectrode breakdown. On account of the small interelectrode gap and the finite dielectric strength of crystals, the amplitude of control pulses was not raised above 20 kV. Up to ± 60 mrad and ± 40 mrad wide deflection of a 2.5 mm wide laser beam was attained with LiNbO₃ or LiTaO₃ crystal pairs and with DKDP crystal pairs respectively, corresponding to a deflector sensitivity of 6 mrad/kV (12 resolvable elements per kilovolt) and 4 mrad/kV (8 resolvable elements per kilovolt) respectively. The results indicate that the deflection angle increases as the temperature is lowered, which confirms the necessity of cooling DKDP crystals for a better performance. Immersion of LiNbO₃ and LiTaO₃ crystals in an appropriate fluid can lower the reflection coefficient from 0.12 to 0.03 and may thus eliminate the need for clearing their faces with special coatings. Figures 4; references 7.

Energy of Subpicosecond Excimer-Laser Pulse Amplification Saturation

917J0102C Moscow IZVESTIYA AKADEMII NAUK
SSSR: SERIYA FIZICHESKAYA in Russian Vol 55
No 2, Feb 91 pp 368-373

[Article by V. T. Platonenko and M. K. Shayakhmetova,
Moscow State University imeni M. V. Lomonosov]

UDC 621.373.826

[Abstract] Amplification of ultrashort ultraviolet radiation pulses in excimer lasers such as the XeCl* and the KrF* is analyzed theoretically on the basis of the Frantz-Nodvik relation (L. M. Frantz and J. S. Nodvik, JOURNAL OF APPLIED PHYSICS Vol 34, 1963) describing the dependence of the output energy on the input energy with the gain and the "amplification saturation energy" as parameters, this relation having been derived for noncoherent radiation but also being used for fitting experimental data on coherent radiation. The response of an excimer molecule to a radiation pulse of duration much shorter than the reciprocal of the half-width of the amplifying B-X transition is described, taking into account transitions from the fixed rotational sublevel j in the vibrational state of the upper term B to the vibrational state v of the lower term X. Linear polarization and circular polarization of light are considered, calculations yielding a higher output energy in the case of circularly polarized light. The amplification saturation energy is, moreover, shown to depend on the nonsaturating losses as well as on both duration and spectral width of the incident radiation pulse, which confirms that the Frantz-Nodvik saturation energy is not an absolute characteristic of an excimer molecule but depends on the conditions of the experiment. References 13.

Compression and Stabilization of Ultrashort Laser Pulses in Periodically Nonhomogeneous Optical Fiber

917J0102D Moscow IZVESTIYA AKADEMII NAUK
SSSR: SERIYA FIZICHESKAYA in Russian Vol 55
No 2, Feb 91 pp 322-328

[Article by V. A. Vysloukh and L. P. Gevorkyan,
Moscow State University imeni M. V. Lomonosov]

UDC 621.373.7

[Abstract] Interaction of picosecond laser pulses propagating in various modes through a periodically nonhomogeneous optical fiber is analyzed, the feasibility of their compression into femtosecond ones being of particular concern. First, compression is considered of a narrow-band wave packet with a spectral width $\Delta\omega \ll \omega_0$ (ω_0 - carrier frequency) and a small frequency-modulation index $m \ll 1$ in a low-directivity two-mode fiber with a periodic longitudinal profile of the refractive index $n(\omega, r, z)^2 = n_0(\omega)^2 [1 + f(r)[1 + m \cos(2\pi z/d)]]$ (n_0 - refractive index of fiber sheath, $f(r)$ - radial profile of the refractive index of the fiber core, d - space period of the refractive index along the fiber axis). Dispersion characteristics and evolution of time envelopes are calculated by the spectral method leading to a pair of independent Schroedinger equations with initial conditions dependent on the excitation mode. Under single-mode excitation such a fiber behaves like a medium with a cubic dispersion, the induced pulse with

a peak-on-pedestal structure being "split" into two partial pulses with equal complex amplitudes "propagating" one through a medium with a normal group velocity dispersion and one through a medium with an anomalous group velocity dispersion. Under symmetric excitation such a fiber behaves like a medium with a normal group velocity dispersion and under antisymmetric excitation it behaves like a medium with an anomalous group velocity dispersion which compresses the induced pulse as a whole. Nonlinear self-compression of strong pulses with a finite spectrum is considered next, disregarding the difference between the effective areas of waveguide modes but taking into account the difference between the cross-modulation coefficients. In this case symmetric excitation produces a pulse with dispersive phase self-modulation in a medium with an anomalous group velocity dispersion, a pulse which diffuses faster than under linear conditions, while antisymmetric excitation degenerates the system into a single nonlinearly dynamic one in a medium with an anomalous group velocity dispersion. Figures 3; references 5.

Generation of Picosecond X-Ray Pulses in Dense Plasma Produced by High-Intensity Femtosecond Laser Pulses of 308 nm Radiation

917J0109A Moscow KVANTOVAYA ELEKTRONIKA in Russian Vol 18 No 3, Mar 91 pp 278-279

[Article by S. A. Akhmanov, I. M. Bayanov, V. M. Gordiyenko, M. S. Dzhidzoyev, S. V. Krayushkin, S. A. Magnitskiy, V. T. Platonenko, Yu. V. Ponomarev, A. B. Savelyev-Trofimov, Ye. V. Slobodchikov, and A. P. Tarasevich, Moscow State University imeni M. V. Lomonosov]

UDC 621.373.826:533.9

[Abstract] Ultrashort pulses of soft x-rays having an intensity of the order of 1 TW/cm^2 and a duration not exceeding 7 ps were generated in a dense metal plasma with an electron concentration of $10^{23} - 10^{24} \text{ cm}^{-3}$, such a plasma having been produced by irradiation of an iron target with 308 nm radiation from an XeCl excimer laser amplifier set in pulses of approximately 550 fs duration so that the energy density at the target surface exceeded 1 PW/cm^2 and 0.5-2 percent of incident light was converted into x-ray quanta with more than 200 eV energy. The main components of the apparatus in this experiment were a dye laser emitting femtosecond pulses of 616 nm radiation, two frequency doublers, and a set of excimer amplifier stages. This scheme ensured excellent pulse characteristics. The dye laser was synchronously pumped by a $\text{YAlO}_3:\text{Nd}^{3+}$ laser with hybrid active-passive mode locking and with negative feedback. This solid-state laser emitted $1.08 \mu\text{m}$ radiation in trains of 500 square pulses, each of 40 ps duration with an amplitude instability not exceeding 2 percent. A part of this radiation was diverted to a selector for extraction of single pulses. These were passed through a solid-state amplifier to one of the two frequency doublers which

then delivered picosecond pulses of 504 nm radiation to the dye laser. The dye laser in turn emitted 616 nm radiation in femtosecond pulses of about 5 nJ energy, single ones coincident in time with the pump pulses being passed through two successive dye-laser amplifiers which delivered them, now with an energy of 150-200 μJ , to the other frequency doubler (KDP crystal). The latter injected 308 nm radiation, in pulses of about 700 fs duration, through a telescope into the the first excimer amplifier stage. In the second stage with a $3 \times 5 \times 6 \text{ cm}^3$ active volume amplification proceeded according to a two-pass scheme, radiation entering at some angle to the cavity axis for the first pass and after filtration covering the entire aperture at the end of the second pass. The second excimer amplifier stage delivered pulses of 550 fs duration and 30 mJ to the target. The conversion of light into x-ray quanta was measured with a pin-diode and its efficiency was found to be 0.5-2 percent. The duration of x-ray pulses was measured with the aid of an x-ray streak camera and interaction chamber set, a filter rejecting quanta of less than 0.3 eV energy having been placed between the target and the camera entrance slit. Figures 1; references 9.

Neodymium-Glass Laser With Two Emission Channels and Continuous Regulation of Time Difference and Tunable Time Delay Between Them

917J0109B Moscow KVANTOVAYA ELEKTRONIKA in Russian Vol 18 No 3, Mar 91 pp 292-294

[Article by N. S. Vorobyev and O. A. Konoplev, Institute of General Physics, USSR Academy of Sciences, Moscow]

UDC 621.373.826.038.825.3

[Abstract] A simple scheme is proposed for a Q-switched neodymium-glass laser with two emission channels and continuous regulation of the time interval between the two pulses over the 0-100 ns range. Synchronization of the channels and Q-switching of the laser are achieved by means of positive crossover feedback through two photomultipliers and two electrooptic crystals. The active medium, a glass: Nd^{3+} rod 100 mm long and 5 mm in diameter, is placed in the optical cavity between a plane 0.5-reflectance wedge mirror and a 0.93-reflectance spherical mirror with a 1.5 m radius of curvature on the common optical axis. A diaphragm with a 1.75 mm hole before the wedge mirror extracts from the reflected beam its transverse mode, which is then split by a birefringent plate of Iceland spar into two parallel orthogonally polarized ones. In this way each emission pulse is split into two, one them being delayed in time and both then being resuperposed in space on the other side of the active medium. Here a Glan-Foucault prism transmits one part of the radiation depolarized in the active medium to the spherical mirror and reflects its other part at a wide angle to an identical other spherical mirror through the thus formed lateral branch of the optical

cavity for the second channel. Feedback is effected through a photomultiplier behind each spherical mirror and an electrooptic crystal, a uniaxial LiNbO_3 crystal of the 3m class, in each cavity-channel between the respective spherical mirror and the prism. Each crystal, a 50 mm long 5 mm square bar, is oriented with its OZ axis along the optical axis of the respective cavity branch with its OX axis parallel to the electric field of the applied feedback signal. The static voltage required by these crystals for frequency doubling of incident $1.06 \mu\text{m}$ radiation is 940 V and 920 V respectively. An electric control device receives signals from the two photomultipliers and sends the feedback signals to the two electrooptic crystals. It consists of a source of bias voltage and a source of adjustable reference voltage which limits the feedback signals, two diodes and two load resistors also being included. The laser is first tuned so that both channels will operate independently in the direct feedback mode, each photomultiplier sending its signal to the electrooptic crystal in its channel. The polarity of the feedback signal can be reversed by reversing the polarity of the bias voltage. Since in the case of positive feedback the radiation emission in the channels depends largely on the amplitude of the feedback signal, each channel is then tuned by regulation of the feedback signal amplitude. The tuned system is then made to operate in the crossover feedback mode, with each photomultiplier feeding its signal to the electrooptic crystal in the other channel so that each channel Q-switches the other one and the two become synchronized. Such a laser was built and tested, the time interval between its two pulses of 80 ± 8 ns duration being measured with an LFD-2 diode and on a Tektronix 466 oscilloscope with an error not larger than about 5 ns. The authors thank I. Ye. Smirnova for assistance in editing the manuscript. Figures 3; references 15.

Two-Stage Shortening of XeCl-Laser Pulse by Stimulated Mandelshtam-Brillouin Scattering

917J0109C Moscow KVATOVAYA ELEKTRONIKA
in Russian Vol 18 No 3, Mar 91 pp 313-315

[Article by M. S. Dzhidzhoyev, S. V. Krayushkin, V. T. Platonenko, and Ye. V. Slobodchikov, Moscow State University imeni M. V. Lomonosov]

UDC 621.373.826.038.823

[Abstract] In an experiment, ultraviolet radiation pulses of about $100 \mu\text{J}$ energy and about 60 ns duration emitted by an XeCl excimer laser were shortened to a duration, not longer than 15 ps, by two-stage stimulated Mandelshtam-Brillouin scattering and then amplified to an energy of about 120 mJ. The laser was operating with truncated Brillouin scattering (TRUBS scheme) by the surface of liquid ethanol. The apparatus consisted of two XeCl electric-discharge stages, the first stage a $\Delta v \approx 0.1 \text{ cm}^{-1}$ amplifier with an active medium filling a 55 cm long cell $0.7 \times 1.8 \text{ cm}^2$ in cross-section and being split into two parallel channels. Its amplifier channel, with a 1 mm

wide diaphragm on each side of the active medium, was located in an optical cavity between a plane high-reflectance mirror and a plane 0.4-reflectance exit mirror, both mirrors slanted at a 45° angle to the optical axis in a V-formation. Into this cavity, before the back mirror, a focusing lens was inserted. Its oscillator channel, also with a 1 mm wide diaphragm on each side of the active medium, was located in an optical cavity between a plane high-reflectance back mirror and a plane 0.5-reflectance exit mirror, both mirrors perpendicular to the optical axis. Into this cavity, before the exit mirror, were inserted two decoupling Fabry-Perot air etalons one behind the other with a 0.1 mm base and a 5 mm base respectively. The active medium of the single-channel second amplifier stage filled a 55 cm long cell $1.2 \times 1.5 \text{ cm}^2$ in cross-section. Without diaphragms, it was located in an optical cavity between a plane high-reflectance back mirror and a plane 0.4-reflectance exit mirror, both mirrors slanted at a 45° angle to the optical axis in a V-formation. Into this cavity, before the back mirror, a focusing lens and attenuating filter were inserted. A plane high-reflectance mirror behind the exit mirror of the oscillator channel cavity transmitted the radiation beam from that channel to a plane 0.30-reflectance second mirror, through a pair of telescoping lenses which narrowed the beam to a 5 mm diameter. This second mirror, parallel to the exit mirror of the amplifier channel cavity, injected the narrow radiation beam, directly, backward into the amplifier channel cavity. It also transmitted radiation from both cavities, through a matching 1:3-magnification telescope formed by another pair of lenses, to the 0.40-reflectance exit mirror of the second stage for backward injection into that stage. Two ethanol cells for stimulated M-B back-scattering were placed outside cavities, one behind the slanted back mirror for the second channel of the first stage and one behind the slanted back mirror for the second channel of the first stage. The lens inside each of these two cavities focused the amplified radiation onto the respective ethanol cell, via that high-reflectance mirror, so as to cause optical breakdown of the liquid surface under a power density reaching the levels up to 10 GW/cm^2 . Pulses leaving the second stage, are shortened and amplified to an energy of 2 mJ, and were further amplified by another XeCl stage with the active medium filling a 60 cm long cell $3 \times 5 \text{ mm}$ in cross-section. This amplifier was operating in the regenerative ring mode, with an optical cavity formed by a X(2-5)-magnification telescope and a $50 \mu\text{m}$ wide diaphragm. Figures 4; references 11.

Accounting for Field Distribution in Optical Cavity When Determining Optimum Transmittance of Exit Mirror

917J0109D Moscow KVANTOVAYA ELEKTRONIKA
in Russian Vol 18 No 3, Mar 91 pp 352-355

[Article by V. A. Malyshev, Institute of Radio Engineering, Taganrog]

UDC 621.373.826

[Abstract] Considering that the optimum transmittance of the laser exit mirror is determined by the condition for steady emission $R_1 R_b h^{2A} = 1$ (R_1 - reflection coefficient of low-reflectance exit mirror, R_b - reflection coefficient of high-reflectance back mirror, L - distance between mirrors, i.e., length of optical cavity, $\alpha = \sigma \Delta n - \alpha_0$ denoting the average over-the-cavity-length gain per unit length of the active medium, σ denoting the cross-section for emission of radiation during their interaction with active particles, Δn - average population inversion of active particles per unit volume, α_0 - coefficient of beam losses in active medium), the laser performance is analyzed in the single-mode monochromatic approximation on the basis of an electric equivalent C-L-G-parallel circuit representing losses in the cavity (thus taking into account its Q-factor) between a conductance representing the useful load and a negative conductance representing the active medium. Taken into account is the radial distribution of the electric field in the cavity, assuming that the laser beam is a Gaussian one. The conditions for optimum transmittance of the exit mirror are established accordingly, whereupon the optimum transmittance along with that average laser gain and also the maximum attainable output power at the exit mirror are calculated for that ideal single-mode monochromatic case. Figures 2; references 6.

Lanthanum Scandoborate: New Highly Efficient Solid State Laser Medium

917J0112A Moscow KVANTOVAYA ELEKTRONIKA in Russian Vol 18 No 2, Feb 91 pp 149-150

[Article by S. A. Kutovoy, V. V. Laptev, S. Yu. Matsnev, Astrofizika Scientific Production Association, Moscow]

UDC 621.373.826.038.825.2

[Abstract] Attempts to develop a new laser material which would make it possible to attain effective absorption within the pump source emission band are described. It is shown that a newly found active laser medium—lanthanum scandoborate $\text{LaSc}_3(\text{BO}_3)_4$ (LSB)—can be activated with Cr^{3+} and Nd^{3+} ions up to 100 percent (i.e., $5.1 \times 10^{21} \text{ cm}^{-3}$) with a distribution factor of unity and 0.7, respectively, without substantial concentrational luminescence quenching, whereby the quantum efficiency of the $\text{Cr} \rightarrow \text{Nd}$ transport amounts to 0.8. The new crystal has a broad transition cross section and effective sensitization and is characterized by neodymium's high stimulated emission efficiency in it. Comparative stimulated emission tests reveal that LSB lasers are two and six times more efficient as YSGG and YAG lasers, respectively (5.4 percent versus 2.6 and 0.76 percent ultimate differential efficiency). Figures 1; tables 1; references 4: 3 Russian, 1 Western.

Repetitively Pulsed 600 W XeCl Industrial Laser

917J0112B Moscow KVANTOVAYA ELEKTRONIKA in Russian Vol 18 No 2, Feb 91 pp 183-185

[Article by V. M. Borisov, A. Yu. Vinokhodov, S. M. Garasimov, Ye. V. Yevstratov, Yu. B. Kiryukhin, S. G. Kuznetsov, Yu. Yu. Stepanov, V. A. Vizir, V. I. Manylov, S. P. Nosenko, S. P. Sychev, V. V. Chervyakov, N. G. Shubkin, Atomic Energy Institute imeni I. V. Kurchatov, Moscow and High-Current Electronics Institute at the Siberian Branch of the USSR Academy of Sciences, Tomsk]

UDC 621.373.826.038.823

[Abstract] A high-power repetitively pulsed XeCl laser with a commercial thyatron-based power supply system capable of attaining a high mean radiating power level is described and its predecessors developed by the Lambda Physik company and other firms are mentioned. The resulting excimer laser is capable of emitting $\lambda = 308 \text{ nm}$ light at a 600 W radiating power. In addition to four commercially produced thyatrons, the laser power supply system contains a magnetic switch. The laser employs automatic ultraviolet (UV) preionization by means of a discharge on a dielectric surface. The results of experiments to develop a hole structure in a polyimide layer applied to an aluminum base with the help of this laser are cited for illustration. It is shown that such a binary film is a flexible medium which can be used for making large-scale integrated circuits. The pump circuit elements' service life is estimated to exceed 10^7 pulses. Figures 4; references 4: 3 Russian, 1 Western.

On Ultimate Duration of Ultrashort Light Pulses Emitted by Passive Mode-Locked Solid State Lasers

917J0112C Moscow KVANTOVAYA ELEKTRONIKA in Russian Vol 18 No 2, Feb 91 pp 207-210

[Article by K. P. Komarov, A. S. Kuchyanov, Automation and Electrometry Institute at the Siberian Branch of the USSR Academy of Sciences, Novosibirsk]

UDC 621.373.826.038.825

[Abstract] The issue of the shape and duration of stationary pulses emitted by solid state passive mode-locked (PSM) lasers is examined without any constraints on the saturable absorber (NP) relaxation time. Principal attention is focused on the hitherto unknown domain of parameters in which the ultrashort light pulse (UKI) duration is short compared to the saturable absorber relaxation time. In so doing, the shape of steady state light pulses and the dependence of their duration on the gain bandwidth, passive filter relaxation time, and its saturation parameter are determined. The outcome of a theoretical analysis is rather consistent with experiments to stimulate emission of picosecond and subpicosecond light pulses. The resulting data make it possible to

evaluate the outlook for mastering the subpicosecond and femtosecond durations while using available saturable absorbers and wide-band solid state gain media. It is shown that by optimizing the parameters of a combined slow- and fast-relaxation saturable absorbers, it is possible further to shorten the duration of light pulses emitted by a neodymium glass laser by 2-2.5 times, reaching a limit of 100 fs determined by the gain bandwidth. The authors are grateful to N. S. Vorobyev, V. A. Babenko, and A. A. Sychev for discussing a range of issues related to the passive mode locking operation of solid state lasers. Figures 2; references 12: 10 Russian, 2 Western.

Laser Plasma Flow Collision With Annular Obstacle and Autoionization Ion State Excitation in Oblique Shock Waves

917J0112D Moscow KVANTOVAYA ELEKTRONIKA in Russian Vol 18 No 2, Feb 91 pp 232-237

[Article by V. A. Boyko, N. P. Datskevich, N. N. Kononov, G. P. Kuzmin, General Physics Institute at the USSR Academy of Sciences, Moscow]

UDC 621.373.826:533.9

[Abstract] The method of spectroscopy with time and space resolution is used to determine the parameters of laser plasma formed on an acrylic plastic target during its scattering and collision with annular obstacles surrounding the focusing area. Excitation dynamics of autoionization states with changes in the buffer gas pressure in the vacuum chamber are examined. The resulting spatial distributions of the electron density and temperature are used to analyze these states' excitation mechanism. A CO₂ laser with an electron beam preionization and a pulse energy of about 1 kJ was used in the experiment which shows that during the collision of the plasma flow with the obstacle, the CII and CIII autoionization ion states are formed in it. The scattering velocities of ions with various ionization ratios are determined both in expanding plasma and during its collision with the obstruction. The development of an oblique shock wave (UV) near the obstacle is examined. It is shown that subsequent studies of the autoionization state formation in the above configuration may be useful for establishing the physical patterns of supersonic multicomponent plasma flow interaction with an obstacle. The authors are grateful to I. L. Beygman and I. V. Sokolov for discussing the results and making constructive remarks. Figures 8; references 13: 8 Russian, 5 Western.

Origins of Cornea and Skin Ablation by Infrared Laser Irradiation

917J0112E Moscow KVANTOVAYA ELEKTRONIKA in Russian Vol 18 No 2, Feb 91 pp 250-253

[Article by N. P. Furzikov, Industrial Laser Science Research Center, Troitsk, Moscow Oblast]

UDC 615.47:621.373.826

[Abstract] Thermal breakdown of soft tissue by the ablation mechanism under the effect of laser irradiation is summarized and a model of ablation of quasihomogeneous soft tissue irradiated by an infrared (IK) laser is proposed. The modeled process involves explosive boiling of superheated water with subsequent thermal breakdowns of the organic tissue frame under the conditions of interferential instability as well as due to the impact of self-absorption. The model adequately describes cornea and skin ablation by infrared laser irradiation using a two-component approximation to real tissue structure. It is shown that a model of a frame half-immersed in a liquid component which is being constantly stripped by pulsed radiation is the most consistent with experimental data. Figures 3; tables 1; references 16: 5 Russian, 11 Western.

Periodically Pulsed Composite Discharge-Pumped Diffusion-Cooled CO₂ Laser

917J0128B Leningrad PISMA V ZHURNAL TEKHNIЧЕСКОY FIZIKI in Russian Vol 17 No 10, May 91 pp 91-95

[Article by A. F. Vitshas, A. N. Kushko, L. P. Menakhin, A. M. Soroka, V. V. Chulkov]

UDC 07

[Abstract] Lasers operating by vibrational-rotational transitions in molecules with diffusion active medium cooling which are characterized by design simplicity and ways of increasing radiating power of gas lasers with convective active medium cooling by using composite discharges where most of the energy is contributed during the recombination plasma decay at a rather low electric field strength/gas pressure ratio while the pulsed discharge with a high E/p ratio is used to develop a high degree of ionization are examined. The possibility of using the combined discharge method to control the pumping of a CO₂ diffusion-cooled laser is studied. In the experiment, conditions for maintaining a non-self-sustained space discharge were realized in a simple laser, making it possible to achieve optimum E/p ratios for the laser's active CO₂ medium excitation conditions and attain periodically pulsed emission with a controlled radiation pulse duration of over 10⁻⁴ and a pulse repetition frequency of 10² to 10³ Hz. The laser medium was ionized by a space discharge. The design of the gas-filled discharge tube and the gas ionization method are described in detail. A peak pulse power of 500 W/m was attained at a 30 torr gas pressure in the tube. It is shown that the peak pulse power is limited by the pump power which, in turn, is limited by the electron concentration in the discharge. Figures 2; references 5: 2 Russian, 3 Western.

Origin of Aromagnetism

917J0086A Moscow PISMA V ZHURNAL
EKSPERIMENTALNOY I TEORETICHESKOY
FIZIKI in Russian Vol 53 No 5, 10 Mar 91 pp 229-232

[Article by M. A. Martsenyuk and N. M. Martsenyuk,
Perm State University imeni A. M. Gorkiy]

[Abstract] Aromagnetism, discovered by N. A. Tolstoy and A. A. Spartakov (PISMA V ZHURNAL EKSPERIMENTALNOY I TEORETICHESKOY FIZIKI Vol 52, 1990) in microcrystals of aromatic substances and manifested in their reorientation when suspended in water or other fluid in a magnetic field, is shown to be a phenomenon of nonmagnetic origin. Their experiments were performed with an alternating external magnetic field and, therefore, actually not the field vector H itself but its time derivative dH/dt equal to $-c(\text{curl } E)$ interacted with these microcrystals. Vector dH/dt being an even one with respect to inversion in space and time, unlike vector H , it will "work" only with particles which have moments of the same parity: axiotoroidal even-even moments G (V. M. Dubovik, L. A. Tosunyan, and V. V. Tugushev, ZHURNAL EKSPERIMENTALNOY I TEORETICHESKOY FIZIKI Vol 90, 1986). Considering that the energy of G - dH/dt interaction is $U = -\lambda G \text{curl } E$ and assuming that moment G of a particle such as an aromatic microcrystal is rigidly coupled to the axis of the particle, the torque acting on such a particle in a magnetic field of intensity H is $K = -\lambda[GdH/dt]/c$. The

angular velocity of such a particle in a viscous fluid and the angular velocity of its rotating axis, assuming a negligible inertia, are $gQ = -\lambda[GdH/dt]/c$ and $de/dt = [e\Omega] = -gl(e[dH/dt])/c$ respectively. It is now proved that molecules of aromatic substances have constant toroidal moments. In accordance with Dewar's MOLCAO method, the orbital $\Psi(r)$ of such a molecule is expressed as a linear combination of s and p orbitals of all carbon atoms in the benzene ring and σ orbitals of all hydrogen substitutes X_A : $\Psi(r) = \sum_a [s_a \phi_s(r_a) + (p_a r_a) \phi_p(r_a)] + \sum_A q_A \sigma_A(r_A)$ (radii-vectors r_a and r_A read from the centers of respective atoms; s_a, p_a, q_A - coefficients). Overlap of orbitals of neighboring atoms are disregarded, in the first approximation, and a planar molecule of an aromatic substance is assumed to have a D_{6h} symmetry. It is then demonstrated that such a molecule has an axiotoroidal moment normal to its plane, its carbon atoms in the $\Phi_{E(2g)}$ state having dipole moments. Since interaction of electric dipoles facilitates "ferromagnetic" ordering of axiotoroidal moments in a crystal lattice, it follows that planar molecules in a given packing will, by interaction of their axiotoroidal moments, become aligned parallel to one another and thus form an ordered "ferromagnetic" or "weakly ferromagnetic" lattice in a microcrystal. It is further noted that aromatic substances form crystals of monoclinic or triclinic class, readily undergoing transition to an axiotoroidally ordered state. The temperature at which this transition occurs can be determined from their dipole-dipole intermolecular interaction energy. Figures 1; references 5.

Excited Muonium Atom State in Condensed Nitrogen

917J0089C Kharkov FIZIKA NIZKIKH
TEMPERATUR in Russian Vol 17 No 1, Jan 91
pp 122-124

[Article by V. G. Grebennik, V. N. Duginov, V. A. Zhukov, B. F. Kirillov, A. B. Lazarev, A. V. Pirogov, V. G. Storchak, S. N. Shilov, Joint Institute for Nuclear Research, Dubna and Atomic Energy Institute imeni I. V. Kurchatov, Moscow]

UDC 539.2

[Abstract] An attempt is being made to determine the state of the muonium atom in condensed nitrogen; in so doing, the state of short-lived muonium in a substance participating in $\text{Mu} + \text{N}_2 \rightarrow \text{N}_2\mu^+$ reaction is determined by measuring the dependence of the muon precession's initial phase ϕ on the perpendicular magnetic field strength. Measurements were taken at temperatures of 28K (α -phase) and 37K (α - β transition area) in nitrogen. The magnetic field strength was manipulated within 0-1,000 Oe. It is established that the relative field stability and nonuniformity within the sample volume were not worse than 10^{-3} . The experiments show that muonium is in an excited state in nitrogen despite the low accuracy with which the phase was determined. It is noted that measurements of remanent muon polarization in condensed nitrogen will make it possible to unambiguously determine the state of muonium in nitrogen and estimate the constant of nuclear hyperfine interaction. The authors are grateful to I. I. Gurevich for supporting the effort, Yu. M. Kagan, N. V. Prokofyev, and M. A. Strzhemechnyy for discussing the results, and V. G. Olshevskiy and V. Yu. Pomyakushin for helping with the experiment. Figures 1; references 6: 2 Russian, 4 Western.

Cold Uranium Fragmentation by Thermal and Fast Neutrons

917J0090A Moscow YADERNAYA FIZIKA in Russian
Vol 53 No 3, Mar 91 pp 621-627

[Article by V. A. Khryachkov, A. A. Goverdovskiy, B. D. Kuzminov, V. F. Mitrofanov, N. N. Semenova, A. I. Sergachev, A. I. Slyusarenko, Physics and Power Engineering Institute, Obninsk]

[Abstract] Binary nuclear fission which is characterized by a wide range of fragment mass and energies complicating the study of this phenomenon is addressed. Consequently, the so-called cold fragmentation (KhF) of nuclei, i.e., a fission method whereby the kinetic energy is close to or equal to the reaction energy, is examined. In this case the neutron emission is forbidden by energy constraints and the mass spectrum of the fragments displays a vivid structure due to shell and pairing effects. Experimental spectra of cold ^{235}U fragmentation induced by thermal neutrons and neutrons with a 1 MeV

energy are presented. Measurements were taken by a paired fragment spectrometer whose operation is based on twin ionization in a chamber with Frisch grids. The experiment was carried out in a KG-2.5 accelerator using a continuous beam. The $\text{T}(p, n)^3\text{He}$ reaction in a solid tritium-titanium target with a depth of 1 mg/cm² on a water-cooled copper base was used as the fast neutron source while thermal neutrons were produced by retarding fast neutrons in a detachable polyethylene 20 cm thick block. A mixture of 90 percent Ar + 10 percent CH_2 was used as the working gas. Four parameters were recorded in the ionization chamber (IK) for each event. It is shown that the nucleus excitation energy at the saddle point is retained by the fragment separation moment; this means that it is impossible to observe cold fragmentation proper of ^{235}U by either (2 MeV) or thermal (1 MeV) neutrons. Figures 8; references 14: 3 Russian, 11 Western.

Iterated Potential Method. Realistic NN-Potential

917J0090B Moscow YADERNAYA FIZIKA in Russian
Vol 53 No 3, Mar 91 pp 680-692

[Article by A. M. Gorbatov, V. L. Skopich, Ye. A. Kolganova, P. V. Komarov, Yu. N. Krylov, V. A. Luchkov, M. I. Marinov, A. V. Bursak, Tver State University]

[Abstract] The iterated potential method (MKV) developed by solving the multiparticle Schroedinger equation and its principal corollary—that excited harmonics are effectively taken into account by complementing the fundamental equation's matrix element (ME) with the so-called genealogical series (GR)—are summarized. Each genealogical series term represents the contribution of a certain generation of angular potential functions (UPF) and is a fractional rational function of the means of various potential powers for the fundamental harmonic. The possibilities of the iterated potential method in the case of "real" fermion systems (realistic interaction among particles) are tested with the help of calculations of the ^{16}O system using various versions of realistic NN-potentials; in so doing, the angular potential function method and pairing correlation operators are used. The genealogical series is checked for convergence using the example of Malfliet-Tjon central potential. At the same time, the mathematical technique for making microscopic calculations is improved and new equations are suggested for correlators in odd states. Furthermore, the method of leading terms is adapted for the first time to computing heavy p -shell nuclei in the angular potential function basis. The scaling functions method is used to solve the hyperradial system of differential equations; the concept of pairing potential correlation (OPK) self-consistency is employed. The calculations show that the MKV method accuracy remains rather high even in the case of rigid potentials. Figures 5; tables 4; references 16: 9 Russian, 7 Western.

Study of Leading s-Quark Hadronization During Inclusive $K^{*0}(892)^-$ and K^0 -Meson Production on Nuclei

917J0090C Moscow YADERNAYA FIZIKA in Russian Vol 53 No 3, Mar 91 pp 796-803

[Article by Yu. A. Kulchitskiy, Joint Institute for Nuclear Research, Dubna]

[Abstract] General hadron-nucleus interactions in high-energy physics are examined and the notions of space-time screening of color charges, i.e., parton hadronization in a nuclear medium leading to a nontrivial nuclear screening of peripheral interaction in the beam fragmentation area in these reactions, are checked. The processes of inclusive $K^{*0}(892)^-$ and K^0 -meson production in K^+A interactions at an 11 GeV energy are analyzed and contributions of $K^{*0}(892)$ -mesons produced in diffraction processes as well as $K^{*0}(892)^-$ and K^0 -mesons formed due to the resonance decay to these reactions are determined. Cross-sections of $K^{*0}(892)^-$ and K^0 -mesons produced directly in the kaon-nucleus interaction are studied in the framework of a model which takes into account the screening of color, hadron production length, and interaction of the not-yet-formed hadron state with the nuclear medium during the leading quark hadronization. It is shown that the model is capable of describing invariant cross-section of the processes under study; at energies on the order of 10 GeV, the contribution of planar diagrams to these cross-sections exceeds those of cylindrical diagrams. The observed increasing dependence of the differential cross-sections ratio of $K^{*0}(892)^-$ and K^0 -mesons is attributed to a decrease in the cross-section of K^0 -mesons produced due to the resonance decay and an increase in the cross-section of $K^{*0}(892)$ -meson production due to the diffraction system and resonance decay. The author is grateful to B. Z. Kopeliovich for numerous and constructive discussions. Figures 5; references 18: 6 Russian, 12 Western.

Superstring Z' -Boson and t-Quark Mass

917J0090D Moscow YADERNAYA FIZIKA in Russian Vol 53 No 3, Mar 91 pp 777-781

[Article by V. A. Bednyakov, Joint Institute for Nuclear Research, Dubna]

[Abstract] The task of determining the sixth t -quark's mass is addressed. This quark still cannot be observed directly even with the help of modern colliders and its mass cannot be measured; an indirect mass estimate of ≈ 300 GeV accurate within 30-40 GeV can be obtained by precision analysis of neutral current data. It is shown that by taking into account the additional Z' -boson one can reduce the t -quark mass determined with the help of radiative corrections. For example, given certain legitimate values of the Z' -boson parameters, this mass can be found to be as low as 90 GeV. It is noted that at fixed values of the Z' -boson, errors in finding the mass and weak angle sine are determined primarily by the accuracy of processed data and, consequently, should not differ substantially from those

obtained in other works. It is shown that a detailed investigation of the issue of finding the t -quark mass indirectly calls for an exhaustive precision analysis of data allowing for the Z' -boson. The author is grateful to M. S. Bilenkiy, Yu. P. Ivanov, S. G. Kovalenko, A. A. Pankov, and I. S. Satsunkevich for stimulating discussions. Figures 2; tables 1; references 10.

Crystal Structure and Morphology of Epitaxial Germanium Sillenite Layers Deposited by Reactive Cathode Sputtering

917J0098A Moscow KRISTALLOGRAFIYA in Russian Vol 36 No 2, Mar 91 pp 469-474

[Article by A. N. Ognev, V. N. Kornetov, V. A. Dmitriyev, U. V. Kostysheva, Moscow Energy Institute]

UDC 539.216.2:548

[Abstract] Epitaxial $\text{Bi}_{12}\text{GeO}_{20}$ (BGO) 0.2-20 μm thick layers deposited by reactive cathode sputtering of composite bismuth-germanium targets on single crystal BGO and silicon sillenite $\text{Bi}_{12}\text{SiO}_{20}$ (BSO) substrates with a (100), (110), (111), and (211) orientation are examined. The substrates were heated to a 450-650°C temperature, thus ensuring the formation of germanium sillenite; the sputtering rate was manipulated from 0.3 to 0.8 $\mu\text{m}/\text{h}$ by varying the power input while keeping other sputtering parameters constant. The crystal structure of the resulting layers was investigated by an UEMV-100K electron diffractometer ("reflection test") and URS-50 IM X-ray diffractometer (nonfiltered Fe-radiation). As a result, the possibility of producing homo- and heteroepitaxial germanium sillenite layers by reactive cathode sputtering is demonstrated and the conditions for obtaining mosaic and single crystal 20 μm thick BGO and BSO films are determined. It is established that the temperature, sputtering rate, and substrate orientation have the dominant effect on the germanium sillenite layer microstructure. It is shown that the crystal structure perfection increases with the thickness of epitaxial layers which may be attributed to a drop in mechanical compressive stresses accompanying the epitaxy process due to variations in the film and substrate lattice parameters. The authors are grateful to A.A. Marin, Yu.L. Kopylov, and V.V. Kuch for providing germanium and silicon sillenite crystals. References 17: 10 Russian, 7 Western; figures 4.

Yield of Heavy Quarks in High-Energy Processes

917J0100A Moscow PISMA V ZHURNAL EKSPERIMENTALNOY I TEORETICHESKOY FIZIKI in Russian Vol 53 No 6, 25 Mar 91 pp 276-279

[Article by Ye. M. Levin, M. G. Ryskin, and Yu. M. Shabelskiy, Leningrad Institute of Nuclear Physics imeni Konstantinov, USSR Academy of Sciences, Gatchina]

[Abstract] Estimates of charm quark and bottom quark yields in high-energy pp-collisions are analyzed on the basis of the parton model, which requires correction for multiple scattering of partons with moderate transverse momentum q_T by soft gluons of original hadrons. This correction is, according to the theory of semirigid processes, appreciable for production of charm quarks in collisions with $s^{1/2}$ from about 0.5 TeV up and for production of bottom quarks in collisions with $s^{1/2}$ from about 20 TeV up. With multiple scattering thus taken into account and according to data on muon or J/Ψ -meson yield, the fraction of charm quarks with transverse mass $m_T \leq q_0$ should be smaller and the cross-section for production of B-mesons should be larger. Considering that production of particles with a small transverse momentum q_T is apparently suppressed by a mechanism analogous to the Landau-Pomeranchuk effect, one can assume that 30 percent of all J/Ψ -mesons are produced due to decay of B-mesons while 70 percent of them are produced due to recombination of cc-pairs. The probability of this recombination is then assumed to be proportional to m_T^{-1} , this assumption being consistent with estimates based on the rules of sum in quantum chromodynamics and leading to rather simple analytical expression for the probability of J/Ψ -meson production due to charm quark production. Further estimates along this line indicate that multiple scattering of gluons during production of heavy quarks may influence the cross-section for production of these quarks in collisions with $s^{1/2} \approx 0.5$ -1 TeV energy much more than now thought. In collisions with $s^{1/2} = 1.8$ TeV, moreover, the cross-section for production of bottom quarks in pp collisions should be $\sigma(pp \rightarrow bb) \approx 200 \mu\text{b}$. Figures 2; references 8.

Mechanism of Steel Hardening by Cyclic Treatment With Low-Energy High-Current Electron Beam

917J0105C Leningrad PISMA V ZHURNAL
TEKHNICHESKOY FIZIKI in Russian Vol 17 No 5,
12 Mar 91 pp 89-93

[Article by V. I. Itin, I. S. Kashinskaya, S. V. Lykov, G. Ye. Ozur, D. I. Proskurovskiy, and V. P. Rotshteyn, Institute of High-Current Electronics, USSR Academy of Sciences, Tomsk]

[Abstract] The results of an experiment involving treatment of carbon steels with a low-energy high-current electron beam in a cyclic sequence of pulses indicate that surface hardening of these steels is effected by cyclic action of stress waves and by the attendant quasi-static residual stress field. In the experiment specimens of grade-45 plain carbon steel and U7A, U12 straight-carbon tool steels, as cast or after prior quenching, were treated with such an electron beam in pulses of 10-20 keV average energy and 0.15 - 1.2 μs duration, its energy density thus being varied over the 0.6 - 6.0 J/cm^2 range. The electron gun generating this beam had an explosive-emission cathode and a plasma-layer anode. One shot was found to produce an approximate 200 μm thick case

within the surface layer of quenched martensitic carbon steel, a case consisting of two zones with the microhardness peaking to a higher maximum at about 50 μm below the surface and to a lower maximum at about 150 μm below the surface. Both maxima exceeded the microhardness of quenched steel prior to electron-beam treatment. As more shots were applied and the energy density W increased, the higher microhardness peak reached the maximum level of 1800 kgf/mm^2 after 300 shots at 15 s intervals raising the energy density to the $W = 2.5 \text{ J}/\text{cm}^2$ level. As the interval between shots was stepwise lengthened to 60 s, the maximum microhardness correspondingly decreased but the thickness of the case increased. The degree of hardening depended moreover on the temperature at which the steel had been tempered prior to electron-beam treatment, steel tempered at a higher temperature being less hardened by this treatment. An analysis of the hardening process and its anomalies, based on direct measurements and numerical calculations, indicates that action of a low-energy high-current electron beam generates bipolar stress waves consisting of compression and rarefaction pulses, the duration of these pulses being comparable with that of the electron beam pulses. Their amplitude in this experiment covered the 1-2.5 GPa range and thus could have exceeded the dynamic yield point of quenched carbon steel. The thickness of the heat-affected zone did not exceed 15 μm , while x-ray phase analysis revealed an about 20 % higher austenite content within an up to 10 μm thick layer. The thickness of the case thus exceeded by far the thickness of the heat-affected zone and even much more so the about 1 μm depth of electron penetration. The hardening effect of such an electron-beam treatment evidently depends on the profile of those bipolar stress waves. Excessive energy density above 2.5 J/cm^2 , moreover, raises the surface temperature of the steel above its melting point so that even evaporation of the steel may begin and maximum microhardness may shift from the upper zone to the lower zone of the case. Figures 2; references 6.

New Kind of Nonexchange Surface Spin Waves in Planar Ferrite-Dielectric-Ferrite Structure

917J0110C Leningrad PISMA V ZHURNAL
TEKHNICHESKOY FIZIKI in Russian Vol 17 No 6,
26 Mar 91 pp 79-81

[Article by S. V. Tarasenko]

[Abstract] Formation of notched nonexchange surface spin waves in a ferrite-dielectric-ferrite structure with a solid dielectric interlayer rather than air is analyzed, taking into account not only the magnetostatic interaction with attendant formation of notched nonexchange surface spin waves but also the magnetoelastic interaction. That the latter interaction can give rise to a new kind of notched nonexchange surface spin waves is demonstrated theoretically on such a structure with an acoustic contact at each ferrite-dielectric boundary. Inasmuch as exchange amplification of magnetoelastic

effects and attenuation of magnetic-dipole effects simultaneously take place where a ferrite is magnetically compensated, a ferrite with fine magnetic compensation is considered: one having one axis of easy magnetization and two sublattices with unequal magnetization vectors. These new nonexchange surface spin waves are shown to be of elastostatic rather than magnetostatic nature, formed by hybridization of nonexchange surface spin waves in the magnetic layers as a result of indirect interaction through quasi-static elastic-strain field in the dielectric interlayer. Acoustic contact between the non-magnetic dielectric interlayer (medium 1) and the magnetic layers (medium 2) ensuring a finite nonzero ratio of their shear moduli μ_1/μ_2 is necessary for formation of these new waves, elastostatic notched spin waves possibly not being formed when that ratio of shear moduli approaches zero. References 7.

New Efficient Isotope Separation Method

917J0113A Leningrad PISMA V ZHURNAL
TEKHNICHESKOY FIZIKI in Russian Vol 17 No 6,
Mar 91 pp 13-16

[Article by B. S. Akshanov, N. A. Khizhnyak, Kharkov Engineering Physics Institute at the Ukrainian Academy of Sciences]

[Abstract] Traditional isotope separation methods are summarized and their drawbacks are examined. Recently developed new combined devices in which high-frequency or pulsed fields are used alongside static magnetic fields (employing resonance phenomena in plasma, pulsed laser fields, etc.) being touted by their manufacturers and their shortcomings are addressed. The disadvantages of the above systems prompted the authors to design a new and rather efficient electromagnetic isotope separation method using relatively simple and inexpensive devices whereby in contrast to all known methods, the change in the trajectory character of charged particles passing through the zero magnetic field plane is employed. The axial magnetic field formed by two coaxial solenoids with antiparallel magnetic fields used in the device, i.e., a magnetic trap with antiparallel magnetic fields, is considered and its principal advantage—versatility—is emphasized. It is stressed that the unit can be easily automated and that there should be a need to attain higher dispersion, the drift space for ions with helical motion may be extended. Figures 2; references 7: 5 Russian, 2 Western.

Slab Projection by Explosion

917J0114A Moscow VESTNIK MOSKOVSKOGO
UNIVERSITETA: MATEMATIKA, MEKHANIKA
in Russian Vol 1 No 2, Mar-Apr 91 pp 39-45

[Article by V. I. Bogdanov, A. V. Zvyagin]

UDC 539.374.4

[Abstract] Explosion-driven projection of an elastoplastic round slab of finite dimensions toward a rigid

gas-filled target is considered. The effect of the slab's strength properties on the throwing process when it is projected toward a gas-filled target is analyzed and compared to data obtained by other authors. A perfect polytropic gas is selected as the gas model since the problem of joint motion of an elastoplastic body in a chamber of complicated configuration is being solved; it is solved in an axisymmetric formulation using numerical methods. In so doing, a universal software package for selecting the chamber configuration, slab dimensions, and its force loading method is developed. The slab is accelerated by detonating an explosive (VV) layer of finite thickness. The slab material is simulated by an elastoplastic Prandtl-Reis medium. It is shown that in the case of explosion throwing into constricting chambers, the slab shape largely depends on the material strength characteristics and the chamber and slab configuration; the effect of gas on the slab motion is negligible while gas dynamic characteristics are determined by both the slab velocity and its shape; consequently, the slab can be simulated by a plane or membrane only after the contact point reaches supersonic motion relative to shear waves. It is demonstrated that gas parameters can be calculated by an individual routine which takes into account real slab motion characteristics, including its shape. The resulting software package is suitable for efficiently analyzing the process of impulse forging and high-speed throwing. Figures 3; tables 2; references 11.

High-Power Soft X-Ray Flux Generation in 'Angara-5-1' Unit

917J0119C Moscow ZHURNAL
EKSPERIMENTALNOY I TEORETICHESKOY
FIZIKI in Russian Vol 99 No 4, Apr 91 pp 1133-1148

[Article by V. D. Vikharev, S. V. Zakharov, V. P. Smirnov, A. N. Starostin, A. Ye. Stepanov, M. V. Fedulov, V. Ya. Tsarfin, branch of Atomic Energy Institute imeni I. V. Kurchatov]

[Abstract] The possibility of reducing thermonuclear targets by exposing them to high-power soft x-ray beams in order to investigate applications of thermonuclear fusion is addressed and the efficiency of converting electric energy into the kinetic energy of collapsing multiwire liners is examined. The characteristics of plasma's soft x-ray emission are analyzed and compared using the Angara-5-1 multimodule system where sets of aluminum, copper, or tungsten wires as well as supersonic annular gas jets were used as the liner load. The experiments were carried out at a 6 TW output level in a complex consisting of eight identical modules executed on the basis of a double water-insulated forming line operating into a common load. The RMS operation spread of the eight modules did not exceed 12 ns. The spectrum-time and space-energy responses obtained theoretically and experimentally are compared and the patterns of multiwire assembly acceleration compactness irregularity caused by the precursor effect are established. The efficiency of kinetic energy conversion into radiation is close to 100 percent. The authors are grateful

to A. Yu. Sechin, V. A. Makhrov, A. V. Kovalenko, and Yu. K. Zemtsov for help with numerical simulation. Figures 12; tables 1; references 21: 18 Russian, 3 Western.

Photoexcited Electron Momentum Alignment and Spin Orientation in Quantum Wells

917J0119D Moscow ZHURNAL
EKSPERIMENTALNOY I TEORETICHESKOY
FIZIKI in Russian Vol 99 No 4, Apr 91 pp 1202-1214

[Article by I. A. Merkulov, V. I. Perel, M. Ye. Portnoy, Engineering Physics Institute imeni A. F. Ioffe at the USSR Academy of Sciences]

[Abstract] Momentum alignment of electrons produced during the interband absorption of plane polarized light in GaAs semiconductor and spin orientation in the case of circularly polarized light are investigated. The momentum and spin distribution function of photoexcited electrons in a quantum well pumped by polarized light normally incident upon the heterostructure plane is found. A simple case of an infinitely deep symmetric well is examined in order to determine the main patterns of the effect while the absence of an inversion center in GaAs crystals is ignored. It is shown that given a small mass ratio of light and heavy holes, the momentum alignment speed increases abnormally and the electron spin orientation decreases with an increase in the electron motion energy in the well plane. The dependence of the plane and circular hot luminescence polarization at its short wave edge on the exciting photon energy is established. The authors are grateful to M. I. Dyakonov and D. N. Mirlin for discussing the results and holding stimulating discussions and to P. L. Roskin for help with calculations. Figures 7; references 18: 8 Russian, 10 Western.

Neutron Resonance Examination and Search For Unusual Excited States

917J0122A Moscow YADERNAYA FIZIKA in Russian
Vol 53 No 4, Apr 91 pp 883-887

[Article by G. V. Muradian, Atomic Energy Institute imeni I. V. Kurchatov]

[Abstract] The possibility of investigating nuclear levels in an energy range where their density may reach a high value of about 1 eV^{-1} by means of neutron spectrometry and the relationship between the neutron resonance and nuclear states are discussed. The possibility of obtaining new data on neutron resonances in order to search for excited states of nuclei displaying unusual properties is considered and the characteristic features of these states are summarized. It is shown that excited states which lead to nonstatistical phenomena in neutron resonances but could not be detected and identified in earlier research may exist. The design of experiments aimed at detecting these states is examined and the γ -ray cascade spectrometer (GKS) used for this purpose is described.

The experiments demonstrate that studies of neutron resonances with the help of γ -ray cascade spectrometers make it possible to obtain new data on compound states and search for highly excited states with unusual properties. References 9: 2 Russian, 7 Western.

Search For Prompt Neutrino Production in pA -Interaction at 70 GeV Energies Using SCAT Bubble Chamber

917J0122B Moscow YADERNAYA FIZIKA in Russian
Vol 53 No 4, Apr 91 pp 999-1004

[Article by V. V. Ammosov, S. V. Belikov, A. P. Bugorskiy, S. N. Gurzhiyev, V. I. Yermolayev, A. A. Ivanilov, P. V. Ivanov, V. I. Konyushko, V. M. Korablev, V. A. Korotkov, V. A. Krupnov, Ye. P. Kuznetsov, A. I. Kurnosenko, V. V. Makeyev, A. I. Mukhin, A. G. Myagkov, A. Yu. Polyarush, Yu. M. Sapunov, Yu. M. Sviridov, A. A. Sokolov, A. V. Uzunyan, High Energy Physics Institute, Protvino]

[Abstract] Experiments based on the total proton beam absorption method with subsequent recording of neutrino and muons produced by half-lepton decays of short-lived particles which greatly contributed to the study of charmed particle production in proton-nucleus interactions are discussed. An attempt is made to search for prompt neutrino production in pA -interactions at a primary proton energy of 70 GeV using a SCAT bubble chamber (PK) filled with freon bromide as the detector. The design of the experiment conducted in the first half of 1989 in the Serpukhov accelerator is presented. The total proton beam absorption technique was used. Iron nuclei were used as the target. The upper bound of the charmed particle production cross-section is found using data on electron neutrino or antineutrino whose background/effect ratio is roughly 30 times lower than that of muon neutrino or antineutrino. It is shown that the experimental results are consistent with the QCD (KKhD) prediction. Figures 4; tables 2; references 17: 5 Russian, 12 Western.

Search for t -Quarks in Multijet Events at UNK Collider Energies

917J0122C Moscow YADERNAYA FIZIKA in Russian
Vol 53 No 4, Apr 91 pp 1082-1089

[Article by S. R. Slabospitskiy, M. V. Shevlyagin, High Energy Physics Institute, Protvino]

[Abstract] The search for t -quarks and its importance in many of today's high-energy physics problems, especially for measuring its mass and refining the standard model parameters as well as recording Higgs' boson mass is discussed. The process t -quark production in an UNK collider in the pp -collision mode at a beam energy of 3 and 0.4 TeV at $s = 2.2 \text{ TeV}$ with subsequent pure hadronic decay modes which result in six-jet final states is examined. Pure QCD multijet event production processes serve as background processes for the t -quark

production. The possibility of detecting a t -quark signal against the QCD background is analyzed. The t -quark production cross-section is discussed. It is shown that in order to discriminate a t -quark signal in the 100-180 GeV mass range, it is necessary to reconstruct W -bosons with high accuracy and record b -quark jets. Calculations

of matrix element squares of background processes are cited. The authors are sincerely grateful to A. K. Likhoded for his constant interest in the effort and numerous discussions and to V. V. Yezhele, Ye. A. Kozlovskiy, and V. A. Petrov for their stimulating discussions. Figures 4; tables 1; references 16: Western.

Is Fundamental Schroedinger Soliton Stabilized in Its Own Nonlinear Optical Fiber?

917J0091A Moscow *ZHURNAL EKSPERIMENTALNOY I TEORETICHESKOY FIZIKI* in Russian Vol 99 No 3, Mar 91 pp 748-762

[Article by A. V. Belinskiy, Moscow State University imeni M. V. Lomonosov]

[Abstract] Conventionally, an ideal fundamental soliton which satisfies Schroedinger's nonlinear equation is settled in an optical nonlinear fiber without losses over an infinite propagation distance whereby the optical fiber has a cubic nonlinearity and is adequately described by a second approximation of the variance theory. Yet spontaneous noise, appearing during the soliton propagation with periodic amplification to compensate for losses in the fiber, is also amplified and stored. It is demonstrated that a similar trend toward accumulation and amplification is inherent in quantum fluctuations, both phase and amplitude, which are always present in real radiation even in the absence of absorption and/or amplification, i.e., in a perfect optical fiber without losses. A theoretical analysis allowing for possible amplification and losses makes it possible to state this confidently, at least at the initial stage of soliton propagation where the approximations used are definitely legitimate. It is also shown that additive steady-state δ -correlated classical noise displays the same tendency. Certain specific features of femtosecond-long solitons related to the peculiarities of their photon statistics during their detection and the need to take into account third- and higher-order variance terms as well as the finite nonlinear medium response time are noted. The author is grateful to V. A. Vysloukh, A. N. Orayevskiy, and A. S. Chirkin for stimulating discussions. Figures 4; references 28: 18 Russian, 10 Western.

Passive Fiber Optic Magnetic Field Transducer With Frequency Output

917J0094A Leningrad *PISMA V ZHURNAL TEKHNIЧЕСКОY FIZIKI* in Russian Vol 47 No 4, Feb 91 pp 32-35

[Article by A. N. Zalogin, S. M. Kozel, V. N. Listvin, A. V. Churenkov, Moscow Engineering Physics Institute]

[Abstract] Recent advances in the development of passive fiber optic transducers (VOD) of various physical quantities whose sensor represents a microresonator produced by anisotropic etching of silicon are described and it is shown that such transducers' output frequency signal is not distorted by changes in the level of optical power transmitted over the optical fiber. In addition, the sensor may be removed to an area of elevated radioactivity, explosion hazard, or high electromagnetic interference since it contains no current circuits. The development of a fiber optic magnetic field transducer whose microresonator represents a cantilever of soft magnetic amorphous alloy (MMAS) attached on one side is described. The MMAS elasticity modulus changes if magnetic field is applied thus directly converting the

measured quantity into the microresonator's natural frequency and opening up new possibilities for designing passive VOD's of physical quantities. The principles underlying the transducer operation are described. Its peak transduction of 65 Hz/Oe is attained in a bias field of 0.6 Oe developed by a magnet while its sensitivity threshold to magnetic field in the 0.10-10 Hz frequency band is 60 nT. It is noted that the proposed passive magnetic field VOD with a frequency-sensitive output signal may be used for high-precision measurements of small displacements ($<0.1\mu\text{m}$) and current. Figures 2; references 3.

On Limit of Resolution of Intraresonator Laser Spectroscopy Method Using FM Resonances

917J0095A Kiev *UKRAINSKIY FIZICHESKIY ZHURNAL* in Russian Vol 36 No 5, May 91 pp 716-719

[Article by M. V. Danileiko, V. N. Nechiporenko, A. M. Fal, L. P. Yatsenko, Physics Institute at the Ukrainian Academy of Sciences, Kiev]

UDC 821.378.826

[Abstract] The use of lasers whose dependence of power on lasing frequency is characterized by narrow nonlinear resonances, making them suitable for superhigh-resolution spectroscopy due to the possibility of determining the spectra structure of atoms and molecules very accurately, investigate relaxation mechanisms, and measure small quantities of absorbing matter, is described. It is shown that in contrast to traditional absorption saturation (NP) methods, the method of intraresonator frequency-modulation (ChM) spectroscopy makes it possible simultaneously to identify narrow resonances whose formation is facilitated by either NP (NP resonances) or dispersion saturation (ND resonances) in the intraresonator absorbing gas thus significantly increasing the volume of resulting information. The limit of resolution of the intraresonator FM spectroscopy is investigated allowing for transit-time effects and it is demonstrated that in using dispersion resonances, this method's resolution is approximately twice that of absorption resonances. In addition, it is shown that a transition to the transit-time area is accompanied by a less than 2-fold resolution degradation for dispersion resonances and less than 3-fold resolution degradation for the absorption resonance. For the experimentally attainable limit of resolution, this discrepancy increases even further due to a higher signal/noise ratio for dispersion saturation resonances. Consequently, the use of FM dispersion saturation resonances in superhigh-resolution spectroscopy is preferable in the case where it is necessary to attain the limit of resolution. Figures 2; references 5: 4 Russian, 1 Western.

On Mechanism of New Radiation Type Development During Relativistic Electron Channeling in Crystal

917J0096B Tomsk IZVESTIYA VYSSHIKH UCHEBNIKH ZAVEDENIY: FIZIKA in Russian
Vol 34 No 1, Jan 91 pp 99-103

[Article by V. G. Bagrov, I. M. Ternov, B. V. Kholomay, High Current Electronics Institute at the Siberian Branch of the USSR Academy of Sciences]

UDC 537.24:535.23

[Abstract] Experimental data on emission of electron and positron beams at energies of $E = 150$ GeV incident upon a germanium crystal at small angles and the newly discovered radiation characterized by an energy peak in the emission spectrum falling within radiated photons at a $0.85E$ energy are discussed. A new interpretation is suggested for the above type of radiation which is attributed to a new physical mechanism related to the generation of longitudinal oscillations of channeled electrons interacting with a certain effective longitudinal periodic crystal axis field whose cycle is determined by the electron's transverse motion period. The possibility of describing the newly discovered radiation as emission of relativistic electrons in a periodic longitudinal electric field is considered. The characteristics of spontaneous emission of relativistic electrons moving in the axial channeling mode in the crystal are analyzed by quantum electrodynamics methods and compared to various published experimental data. It is shown that on the order of magnitude, the spatial period of electron motion in elliptical orbits in the axial channeling mode coincides with the variation period of the longitudinal electric field for the first radiated harmonic. References 14: 12 Russian, 2 Western.

Spatial Polarization Solitons in Vector Theory of Self-Focusing

917J0102E Moscow IZVESTIYA AKADEMII NAUK SSSR: SERIYA FIZICHESKAYA in Russian
Vol 55 No 2, Feb 91 pp 346-350

[Article by F. N. Marchevskiy, V. L. Strizhevskiy, and Ya. A. Turchin, Kiev State University imeni T. G. Shevchenko]

UDC 621.371.24

[Abstract] Propagation of an elliptically polarized Gaussian light beam through a nonlinear nonmagnetic medium is analyzed by the variational method as a vector problem of self-focusing, the medium assumed to be an isotropic nondissipative one and the electric field of the light beam assumed to have two components $E^{+/-}$ circularly polarized in opposite senses. The corresponding system of two coupled short equations for the Schrodinger wave functions $\Psi^{+/-} = E^{+/-}/E_0$ is solved for appropriate boundary conditions at the entrance to the

medium. The problem reduces to that of finding the vector function $\Psi = e^{+}\Psi^{+} + e^{-}\Psi^{-}$ which will minimize the functional $F = \text{Int}_0^{\infty} \text{Int}_0^{\infty} L dR d\xi$ ($\xi = z/2k_0 a_0^2$, z - longitudinal coordinate, a_0 - radius of E^{+} beam at entrance to medium $z = 0$, k_0 - length of wave vector at frequency ω in the linear approximation, $R = r/a_0$, $r^2 = x^2 + y^2$, x, y - transverse Cartesian coordinates, L - Lagrange function which makes the pair of Euler equations for the derivatives of the wave functions $\Psi^{+/-}$ with respect to ξ and with respect to R coincide with those original two equations). Application of the variational method using equations of the $\delta L^{*}/\rho^{+}$ kind ($L^{*} = \text{Int}_0^{\infty} L dR = L$ averaged over R) leads to a system of nonlinear ordinary differential equations which can be further reduced. These are solved for Gaussian light beams of the same initial intensity but with a different initial ellipticity each and for Gaussian light beams with the same initial ellipticity but of a different initial intensity each, the condition when self-focusing begins being of special interest. The results describe the evolution of such Gaussian light beams and yield the conditions for existence of a spatial polarization soliton, transition from self-defocusing to self-focusing evidently occurring as the ellipticity of the Gaussian light beam is decreased while its intensity is held constant. The self-focusing threshold is, moreover, shown to be about 1.5 times lower than for a linearly polarized Gaussian light beam. Figures 3; references 10.

Evolution of Quantum Fluctuations During Nonlinear Propagation of Fundamental Soliton

917J0102F Moscow IZVESTIYA AKADEMII NAUK SSSR: SERIYA FIZICHESKAYA in Russian
Vol 55 No 2, Feb 91 pp 351-356

[Article by A. V. Belinskiy, Moscow State University imeni M. V. Lomonosov]

UDC 535.14

[Abstract] Propagation of a fundamental soliton through a nonlinear optical fiber is shown to be attended by a buildup of quantum fluctuations, even in the absence of insertion losses when neither attenuation nor amplification occurs. The evolution of a quantum field in a nonlinear optical fiber is described by an equation for slowly varying operators of both positive-frequency and negative-frequency electric field components in the Heisenberg representation, this equation indicating the effects of dispersion and nonlinearity on optical radiation passing through such a fiber. The source of linear losses is assumed to be interaction of optical radiation and an infinite Markov system of phonons. Transformation of one radiation mode whose frequency deviates from the carrier frequency is then characterized by evolution of the Heisenberg operator of phonon annihilation, one term of the derivative of this operator with respect to the longitudinal space coordinate being a random Langevin force. A multimode optical quantum field is considered next, assuming that the absorption

line is uniformly widened but so as not to exceed the width of the signal spectrum. Linear amplification of a signal during stimulated Raman scattering in the third fiber layer is then treated as being analogous to interaction of photons and phonons generated by a pumping laser beam. Analysis and calculations on this basis reveal not only that the dispersion of quantum phase fluctuations increases during propagation of a fundamental soliton through a nonlinear fiber, this increase of their dispersion not being limited by the simultaneous increase of phase indeterminacy, but also that quantum amplitude fluctuations as well as quantum phase fluctuations increase in the process, even when only one fundamental soliton propagates through such a fiber. The author thanks V. A. Vysloukh for stimulating and helpful discussions. Figures 2; references 11.

Fiber-Optic Magnetic Field Strength Microscope

917J0105A Leningrad PISMA V ZHURNAL
TEKHNICHESKOY FIZIKI in Russian Vol 17 No 5,
12 Mar 91

[Article by S. M. Kozel, V. N. Listvin, and A. V. Churenkov]

[Abstract] A fiber-optic magnetic field strength microscope with phase-lock automatic frequency control is described which includes a capillary tube, serving as the probe. This probe, made of fused quartz 5 mm long and 40 μm in diameter, contains a core made of an amorphous alloy and feeds a photodiode. The photothermal effect, intensity-modulated by radiation from a laser diode, is transmitted from the latter through a multimode optical fiber to the probe so as to excite it into flexural vibrations. Its vibrations are recorded contactlessly with a low-contrast Fabry-Perot interferometer, the latter being formed by the probe surface and the exit end face of a single-mode optical fiber from another laser diode. The operation of such a microscope was demonstrated on examination of a magnetic tape and measurement of its normal magnetization component. The tape carried a harmonic signal of an amplitude 10 dB above nominal magnetizing it longitudinally with a space period of about 110 μm . While the probe was being moved over the tape in 10 μm steps, the oscillator frequency varied as a periodic function of the probe displacement along the tape. The lower part of the curve representing this displacement dependence of the oscillator frequency was inverted with respect to the horizontal line at the level of the natural frequency of probe vibrations in the absence of a magnetic field, an indication of an evidently uniform transverse magnetization of the tape. The resolution of this microscope, determined by the dimensions of the probe tip, was about 3 μm . Figures 2; references 4.

Source of Picosecond Pulses From Semiconductor Laser in Fiber Optical Cavity

917J0106A Leningrad PISMA V ZHURNAL
TEKHNICHESKOY FIZIKI in Russian Vol 17 No 6,
12 Feb 91 pp 14-17

[Article I. A. Knyazev, A. S. Shcherbakov, Yu. V. Ilin, N. L. Rassudov, and I. S. Tarasov]

[Abstract] A source of picosecond pulses of 1.3 - 1.6 μm radiation has been built with single-mode InGaAsP/InP double-heterojunction semiconductor laser, the double heterojunctions being separated by an ultrathin active region. An approximately 1 m long optical fiber served as external cavity with movable foccon lens at one end and a mirror at the other. A feedback factor of 0.15 was attained with about 40 percent of the radiation passing through the fiber. Periodic loss modulation in this cavity was effected by injection of a high-frequency alternating current component from an external variable-frequency 400-850 MHz oscillator through a matching strip-line circuit so as to maximize the a.c. input power P, in addition to the 125-140 mA direct current component exceeding the 5-20 mA emission threshold. Stable operation of this pulsed laser at the 1.32 μm wavelength was found to be attainable with the active medium at a temperature within $16 \pm 0.2^\circ\text{C}$. Mode locking at frequencies f exactly or approximately equal to multiples of the 100 MHz frequency separation between cavity modes was found to be feasible so that the emission pulses could be compressed to nearly femtosecond duration: 3.5 ps ($f = 410$ MHz, $P = 1.05$ W), 2.6 ps ($f = 510$ MHz, $P = 1.12$ W), 2.3 ps ($f = 610$ MHz, $P = 1.06$ W), 2.2 ps ($f = 720$ MHz, $P = 95$ W), 2.1 ps ($f = 820$ MHz, $P = 0.87$ W). Such a mode-locking corresponds to circulation of $N = 2nL/c$ light pulses in the fiber cavity (n - refractive index of fiber core material, L - length of fiber, c - speed of light). Figures 2; references 3.

On Possibility of Synthesizing Three-Dimensional Images Using Gaseous Discharge Light Sources

917J0129A Leningrad PISMA V ZHURNAL
TEKHNICHESKOY FIZIKI in Russian Vol 17 No 8,
Apr 91 pp 41-44

[Article by Yu. B. Golubovskiy, I. E. Suleymenov]

[Abstract] The behavior of gaseous discharge light sources in the traveling ionization wave, or strata, propagation mode whereby the strata are regular nonlinear waves with a large amplitude and modulation depth whose wavelength and frequency may vary within a broad range depending on the discharge conditions and type of strata, and the possibility of using this phenomenon for synthesizing images, including three-dimensional ones, are discussed. The possibility of realizing these images by means of representing the integrated radiant intensity in the form of a spatial Fourier series is analyzed. A system of transparent gaseous discharge tubes serving as a three-dimensional screen is considered and, by analogy with TV pictures, each tube is considered as an individual line. It is shown that such a system may be realized by a set of contracted columns; its principal difference from a two-dimensional TV screen is explained. A random luminance intensity along the tube length can be obtained by controlling the discharge current in the domain of time. An analysis of the model demonstrates that images, including three-dimensional, can be synthesized on the basis of stratified gaseous discharge plasma. Figures 1.

Passage of Femtosecond Solitons Through Fiber-Optic Loop

917J0109E Moscow KVANTOVAYA ELEKTRONIKA in Russian Vol 18 No 3, Mar 91 pp 333-336

[Article by E. A. Zakhidov, F. M. Mirtadzhiev, D. V. Khaydarov, A. V. Kuznetsov, and O. G. Okhotnikov, Department of Thermophysics at UzSSR Academy of Sciences, Tashkent, and Institute of General Physics at USSR Academy of Sciences, Moscow]

UDC 681.7.068

[Abstract] A fiber-optic loop is considered for transmission and switching of fundamental femtosecond solitons, such a loop terminating into a fused single-mode directional coupler with two outputs so that it becomes a two-beam interferometer through which two radiation propagate in opposite directions. The performance of such a loop is analyzed theoretically and on the basis of experimental data, considering that a directional coupler is characterized by its division of radiation it feeds into the two ends of the loop: one receiving an α fraction and the other receiving the $1 - \alpha$ fraction. Inasmuch as $\alpha = \cos^2(\pi L/b)$ (L - length of directional coupler, b - beat length for its natural modes) and that the beat length b depends on the radiation wavelength λ , α is a periodic function of λ . First, a single passage of a fundamental soliton is expressed through the directional coupler and the conditions are established for its formation depending on the degree of radiation division symmetry. In a directional coupler with $0.75 > \alpha > 0.25$ solitons form in both its arms and interfere upon their return from the loop, their amplitudes being different and their phase being nonreciprocal unless the directional coupler is symmetric ($\alpha = 0.5$). In a strongly asymmetric directional coupler with $\alpha > 0.75$ or $\alpha < 0.25$ a soliton will form in only one of the arms. Upon its return from the loop, no new soliton with a different envelope will then form and the wave packet will dispersively diffuse. Passage of fundamental solitons through the fiber-optic loop with a linear phase advance is examined next, assuming that the nonlinear phase advance is so small that it does not influence the radiation division factor α . In the experiment with an almost dispersionless directional coupler and a 2 m long fiber-optic loop, 1.55-1.8 μm radiation solitons of 100-200 fs duration were formed during multistage stimulated Raman scattering in a 130 m long homogeneous optical waveguide. A continuously pumped YAG:Nd³⁺ laser, Q-switched and mode-locked, was the source of 1.064 μm radiation emitted in pulses of 150-100 ps duration. The transmission spectrum of the fiber-optic loop was measured and the dependence of its transmittance on the characteristic of the directional coupler, namely the radiation division factor α , then readily calculated in the dispersionless approximation. The authors thank Ye. M. Dianov, F. Kh. Abdullayev, and M. A. Kasymdzhanov for support and fruitful discussions. Figures 5; references 10.

Effect of Aging on X-Ray Optics of Ta/Al Multilayer Interference Structures

917J0110A Leningrad PISMA V ZHURNAL TEKHNIЧЕСКОY FIZIKI in Russian Vol 17 No 6, Mar 91 pp 42-44

[Article by A. G. Lyubimov, Yuen Kshyan-Yang, A. S. Ilyushin, and U Dei-Qing]

[Abstract] An experimental study of Ta/Al multilayer interference structures was made concerning the effect of aging on their x-ray optics, six such structures with alternating Ta and Al layers having been formed in a magnetron chamber: two of them on Si single crystals with a [111] surface orientation and the other four on glass substrates. They were all aged for six months inside a hermetic container at room temperature. Measurements were made in an x-ray diffractometer which included an x-ray tube with a copper anode as source of 0.154 nm radiation and two crystals, one of them oriented so as to cover the range of incidence angles including total internal reflection and one serving as monochromator oriented for symmetric [111] reflection. The incident beam of x-rays was collimated by a diaphragm with a 0.1 mm wide slit. Measurements were made on diffractograms recorded immediately after formation of the structures and after the six month aging period. The fresh structures yielded diffraction patterns with 4-6 interference peaks about 3' wide at half-maximum level and up to 0.70 reflection coefficients in the first order, indications of their high quality. Aging was found to have lowered the reflection coefficients in the first order appreciably to within 0.02 - 0.10 and reduced the peaks in both second and third orders to "staircase tails" to the background level, indications that diffusion had taken place. Incidence at glancing angles of 17-20° yielded patterns with peaks characterizing a polycrystalline structure. Neither the form nor the location of these peaks had changed during aging, an indication that diffusion rather than chemical reactions had caused the degradation of those structures. References 2.

Fractal Dynamics of Deformable Media

917J0110D Leningrad PISMA V ZHURNAL TEKHNIЧЕСКОY FIZIKI in Russian Vol 17 No 6, 26 Mar 91 pp 84-90

[Article by A. S. Balankin]

[Abstract] For an analysis of the dynamics of deformable media, expressions for the bulk modulus B and shear modulus G in terms of their Young modulus E , dimensionality d_r of their fractal structure, and dimensionality of its confining space, also an expression for their Poisson ratio ν in terms of these two dimensionalities, are derived in accordance with the linear theory of elasticity and the self-similarity of fractals. Obviously, with $d = 2$ and $d = 3$ these expressions are identical to those in the linear theory of elasticity for two-dimensional bodies and three-dimensional ones respectively. Considering that Poisson's law not only postulates

transverse strain without transverse stress but also postulates structural stability of a fractal and applies the Le Chatelier-Brown principle to elastic strains, the range of $d - d_f$ is now established within which a fractal will tend to compensate a change of volume δV representing a strain ε_i under a stress σ_i . The corresponding Cauchy relations for regular fractals are, moreover, reduced to the equality $v^{(d)} = 2/(d^2 - 1) = 2v_{\max}/(d + 1)$. A relation is ultimately obtained which describes the dependence of the fractal dimensionality on the dimensionality of the confining space and on the Poisson ratio: $d_f = (d - 1)(1 + \nu) \leq d$. This dependence is then compared with that according to the Witten-Sandier model. The characteristic scale L_m , namely the lower bound for the fractality region of nonuniform fluctuations, determines the smallest scale of density fluctuations in a solid body. Inasmuch as L_m is for most materials much larger than the lattice a -constant, the constant-volume specific heat has a rather small fluctuation component C_v^Φ proportional to T^{d^*} (T - absolute temperature, d^* - spectral dimensionality). A typical material is $MgSiO_3$ with C_v proportional to $T^{2.218}$, here $d^* = 2.218$ being very close to $d_f = 2.23$ calculated according to the theory of fractals. The relation between fractal dimensionality and critical parameters of a material such as the critical stress yields values of these parameters which differ from their values obtained on the basis of the applicable mean-field theory, the discrepancy very likely being due to violation of the Cauchy conditions and to disregard long-range correlations at the percolation threshold in the mean-field theory. Under stresses higher than critical the energy imparted to a deformable medium concentrates in regions far off equilibrium and distributed over the volume of the medium in the form of fractals, which facilitates efficient subsequent energy transfer and explains the experimentally observed turbulence of large plastic deformations. At the bifurcation point, which defines the maximum and thus critical strain $\varepsilon_{cr} = (d - 1)/2d_f$, the system of fundamental equations of the theory of elasticity in Lagrangian coordinates ceases to be an elliptic one and becomes a hyperbolic one. Considering the relation between the fractal dimensionality and Lyapunov's stability exponents, an expression is obtained for the dimensionality D_f of those regions in a plastically deformable medium where excess energy concentrates. Fracture of such a material is considered next, the condition for brittle fracture being $D_f - d_f \ll 1$ (excess energy concentrated near fracture site) and the condition for ductile fracture being $4 < D_f < 40$. Fracture can be quasi-brittle or quasi-ductile when $3 \leq D_f \leq 4$ and a material becomes superplastic when $D_f > 40$. In the case of a D_f -dimensional sphere with a radius L_f , its calculated surface area S_f and volume V_f yield a D_f equal to the similarity coefficient which defines the hierarchy of structural scale factors characterizing deformation and fracture levels. The thus determined values of D_f agree closely with its values obtained by empirical calculations for a geophysical medium subject to seismic events and with its values obtained experimentally. The results of this broad analysis indicate that all open systems eventually acquire a hierarchical multifractal

structure which provides the optimum conditions for energy, mass, and entropy exchange with the ambient medium, this conclusion having been confirmed by the results of geophysical and astrophysical studies. Tables 1; references 26.

Stimulated Diffuse Nanosecond Pulse Backscattering in Cumulative Exposure Mode

917J0119A Moscow ZHURNAL EKSPERIMENTALNOY I TEORETICHESKOY FIZIKI in Russian Vol 99 No 4, Apr 91 pp 1082-1087

[Article by I. V. Gusev, B. Ya. Zeldovich, V. A. Krivoshechekov, V. V. Shkunov, Electrophysics Institute at the Urals Branch of the USSR Academy of Sciences]

[Abstract] Stimulated diffuse scattering (VDR) backward under cumulative exposure conditions with phase conjugation in $LiNbO_3:Fe$ crystals is examined for a train of $\lambda = 0.53 \mu m$ nanosecond second harmonic pulses of a YAG:Nd laser emitting in a pulse repetition mode at a $\nu \leq 0.5$ Hz frequency. The efficiency of periodic pulsed recording was examined for a process which represents two-wave amplification of a weak counter-propagating signal beam initiated in the crystal itself by spontaneous pump beam scattering on crystal defects in the pump beam field. Energy transfer between counter-propagating waves due to stimulated diffuse scattering on photorefractive lattices which grow under the periodic pulsed exposure is investigated and the condition of exposure accumulation is established. The experiments confirm the theoretical possibility of phase conjugation and show that the efficiency of lattice recording within the range of pulsed periodic exposure depends on the current exposure density. It is shown that under such exposure conditions, diffuse backscattering may occur in the cumulative exposure mode with an exposure density threshold of $\approx 10^3$ J/cm². Figures 2; references 12: 4 Russian, 8 Western.

Vector Envelope Soliton Bifurcation and Hamiltonian System Integrability

917J0119B Moscow ZHURNAL EKSPERIMENTALNOY I TEORETICHESKOY FIZIKI in Russian Vol 99 No 4, Apr 91 pp 1113-1120

[Article by V. M. Yeleonskiy, V. G. Korolev, N. Ye. Kulagin, L. P. Shilnikov, Physical Problems Research Institute imeni F. V. Lukin]

[Abstract] The need to analyze soliton-type solutions of systems of nonlinear Schroedinger equations necessitated by modern research into optical solitons in fiber optic waveguides allowing for birefringent properties of the nonlinear medium or the finite number of waveguide modes is addressed. The problem of branching bifurcations, i.e., production and annihilation, of stationary vector envelope solitons under the effect of solitons with a given polarization produced by changes in structural parameters is examined. The relationship of these types

of bifurcations with the integrability of the dynamic system with two degrees of freedom resulting from the reduction of a system of nonlinear Schroedinger equations is discussed. The possibility of using these branching bifurcations for controlling the soliton signal structure is analyzed. Figures 2; references 7: 5 Russian, 2 Western.

Nonclassical Bichromatic Field-Induced Optical Effects

917J0120A Moscow *ZHURNAL EKSPERIMENTALNOY I TEORETICHESKOY FIZIKI* in Russian Vol 99 No 5, May 91 pp 1416-1430

[Article by G. Yu. Kryuchkan, Physical Research Institute at the Armenian Academy of Sciences]

[Abstract] Properties of quantum states of light as well as various ways of producing them are discussed. Statistical properties of nonclassical light obtained during the interaction of a system of atoms with a nonmonochromatic bimodal intense laser field in an optical resonator are investigated. Mode frequencies are symmetrically positioned relative to the atomic transition frequency. A quantum electrodynamic theory of resonance fluorescence and interatomic correlation in the bichromatic field is developed allowing for multiphoton processes and vacuum radiation fluctuation and relaxation effect. The coefficient of nonlinear absorption of the mode by the atomic medium and light intensity on the resonator output are calculated; both figures differ significantly for those of the monochromatic field. The standard deviation of quadrature amplitudes and correlation intensity functions are calculated in the cases of unimodal and bimodal excitation in the resonator. It is shown that the central fluorescence line frequency mode is excited in the squeezed state with suppressed quantum fluctuations of the quadratic amplitude as a result of which there is an intensity interference displaying a nonclassical photon superbunching property. Thus, the possibility of generating a light field in a unimodal squeezed state is demonstrated. The author is grateful to the participants in the Physical Research Institute seminar and especially K. V. Kheruntsyan for discussing the work. Figures 5; references 23: 8 Russian, 15 Western.

Charge Density Wave Dislocations in Crystals

917J0120B Moscow *ZHURNAL EKSPERIMENTALNOY I TEORETICHESKOY FIZIKI* in Russian Vol 99 No 5, May 91 pp 1539-1550

[Article by S. A. Brazovskiy, S. I. Matveyenko, Theoretical Physics Institute imeni L. D. Landau at the USSR Academy of Sciences]

[Abstract] Dislocation mechanism of charge density wave (VZP) motion is discussed. The phase deformation, charge, and Coulomb potential distribution in the medium around the soliton cluster are established and the dependence of the system energy on the $2N$ charge

where N is the number of aggregated 2π -solitons is investigated. The cluster energy as a function of the number of solitons is found and interactions of microscopic solitons and electrons with gas are considered in the framework of the macroscopic theory of dislocations. According to this theory, the phase 2π -soliton can be considered as a microscopic dislocation loop lying in a plane perpendicular to the chain axis. In particular, soliton dislocation and aggregation in charge density wave crystals is examined at low temperatures; the principal phenomena discovered in the study are attributed to Coulomb interactions of residual carriers at low temperatures. It is shown that in the presence of electrons and solitons, screening effects become significant. The results point to successive stages of current conversion in charge density wave crystals. The energy of a plane circular loop is calculated. References 22: 6 Russian, 16 Western.

Three-Wave Interaction in Semiconductors Due to Exciton-Biexciton Mechanism: Additional Boundary Value Condition Problem and Three-Frequency Solitons

917J0120C Moscow *ZHURNAL EKSPERIMENTALNOY I TEORETICHESKOY FIZIKI* in Russian Vol 99 No 5, May 91 pp 1579-1597

[Article by A. L. Ivanov, V. V. Panashchenko, Moscow State University imeni M. V. Lomonosov]

[Abstract] Optical manifestations of the exciton-biexciton Stark-effect, especially elementary excitation spectra modifications leading to effective modification of optical semiconductor characteristics in the exciton resonance region in the presence of a pump wave, are examined. To describe the change in the semiconductor's optical properties in the presence of given pumping, a system of macroscopic equations is derived for the electromagnetic field and exciton and dipole-inactive polarization which are components of the probing radiation, and relevant Poynting's theorem is considered on the basis of these equations. Expressions are also derived for the total probing wave flux. The problem of additional boundary value conditions (DGU) is formulated and analyzed for the system of macroscopic equations. A DGU set which meets the continuity requirement of the total energy flux through the crystal boundary is suggested and expressions are derived for the reflection spectra of probing electromagnetic radiation allowing for the possibility of introducing exciton and biexciton "dead" layers. The total set of nonlinear macroscopic equations is analyzed in the case of comparable probing and pump wave intensities and its three-wave soliton solutions are considered. A consistent method of finding soliton solutions is developed; it is characterized by the need to take the polariton effect precisely into consideration. It is shown that the resulting soliton solutions principally differ from conventional results of nonlinear optics in that the proposed approach makes it possible to analyze the case of the dark soliton appearance at one polariton frequency whereas it is usually assumed that a

dark soliton may form only on a maximum frequency wave; in this case the dipole-inactive biexciton polarization wave which probably cannot be used as a pump wave serves as such a maximum frequency wave. Figures 8; references 16: 8 Russian, 8 Western.

Optically Controlled VO₂ Film-Based Fiber Switch

917J0124A *Leningrad PISMA V ZHURNAL
TEKHNICHESKOY FIZIKI in Russian Vol 17 No 9,
May 91 pp 81-85*

[Article by F. A. Yegorov, Yu. Sh. Temirov, A. A. Sokolovskiy, V. F. Dvoryankin]

[Abstract] Properties of metal-semiconductor phase transitions (FP) in a VO₂ film on the optical fiber end which can be easily induced by optical radiation at a relatively low power of 2 mW, opening up prospects for developing various fiber optic elements controlled by

optical radiation, are discussed. The results of a study aimed at developing an optically controlled fiber switch (OUVP) on the basis of VO₂ films are presented. The phase transition transmission and reflectance can be manipulated by selecting the thickness of the film which serves as the switching element. Two switch design versions are described. An experimental prototype employing multimode Y-couplers operating on a $\lambda \approx 1.6$ μm wavelength was developed. Estimates show that a VO₂ film grown on the end of an optical fiber with a 60 μm diameter, used as a switch, has a response speed of close to 100 μs . The switch is simple, easy to manufacture, and exceeds known thermal optical switches with respect to its response speed and control power yet its losses are rather high (close to 10 dB). The switch may also be realized by using single-mode optical fibers in which case the control power does not exceed 1 mW while the actuation time is at least ten times shorter than that obtained in multimode fibers. Figures 2; references 6: 5 Russian, 1 Western.

Plasma in Intense Sound Wave Field

917J0092A Moscow AKUSTICHESKIY ZHURNAL
in Russian Vol 37 No 2, Mar-Apr 91 pp 213-221

[Article by A. R. Aramyan, G. A. Galechyan, A. R. Mkrtchyan, Applied Physics Problems Institute at the Armenian Academy of Sciences]

UDC 531

[Abstract] The results of an experimental investigation of the effect of the intensity of a standing sound wave propagating along the plasma column on the discharge parameters are cited and it is shown that at a constant gas pressure in the chamber, an increase in the sound wave intensity leads to a decrease in the discharge current, a rise in the electric field strength, an increase in the energy contribution to the discharge, positive discharge column pinching, and an increase in heat extraction along the tube radius. Experimental data demonstrate that the effect of plasma column expansion increases with the discharge current, i.e., an increase in the temperature gradient along the tube radius; as a result, a more uniform gas temperature and pressure distribution in the discharge radius is observed, leading to a more uniform ionization frequency distribution in the tube cross-section and, consequently, a uniform filling of the discharge chamber with plasma. It is also shown that the appearance of acoustic turbulence may lead to the discharge pinching. Figures 9; references 16: 10 Russian, 6 Western.

On Some Relaxation Behavior Anomalies of Supercooled Liquids Based on Acoustic Experiment Data

917J0092B Moscow AKUSTICHESKIY ZHURNAL
in Russian Vol 37 No 2, Mar-Apr 91 pp 235-245

[Article by A. A. Berdyyev, A. V. Rudin, V. M. Troitskiy, Engineering Physics Institute at the Turkmen Academy of Sciences]

UDC 534.8-537.2

[Abstract] Relaxation properties of condensed media are examined from the viewpoint of analyzing the mechanisms of molecular mobility and developing a universal theory of liquid state with respect to tribological applications where rheological properties of lubricants which largely determine the friction coefficient, permissible load, and net power transmitted in friction gears through the lubricant layer are taken into account in engineering analyses. Experimental data on acoustic parameters of seven supercooled liquids, e.g., polyesters and mineral oils, within a 3-90 MHz band, a 363-223K temperature range, and a 0.1-200 MPa applied pressure range are cited. The temperature and pressure dependence of the structural relaxation time of the liquids under study is determined. Experimental data and analyses show that the contribution of the low-frequency relaxation process

to the behavior of volume viscosity can largely explain the discrepancy between experimental and theoretical plots of longitudinal pliability while the effect of the process on the behavior of shear viscosity is insignificant but quite recordable. Figures 5; tables 1; references 29: 16 Russian, 13 Western.

Using New Approaches to Compute Scalar Wave Field's Scattering Coefficient of Statistically Rough Surface With Complex Spectral Composition

917J0092C Moscow AKUSTICHESKIY ZHURNAL
in Russian Vol 37 No 2, Mar-Apr 91 pp 270-276

[Article by M. Yu. Galaktionov, Acoustics Institute imeni N. N. Andreyev at the USSR Academy of Sciences]

UDC 551.463.21

[Abstract] The issue of wave (including acoustic) diffraction on a rough surface is addressed and two traditional ways of analytical approach to this problem—the perturbations method (MMV) and quasiclassical tangential plane approximation (PKV or Kirchhoff's method) are summarized. A new approximate expression suggested by A. G. Voronovich for calculating the scattering pattern of a wave field on a statistically rough surface with a complex spectral constitution is used for cylindrical and isotropic surfaces. Main sections of the indicatrix of diffusion are calculated. An agitated sea surface with a complex spectral composition modeled by a normal centered spatially uniform statistical elevations ensemble was used as an example of statistically rough surface for computer analyses. Statistical properties of the ensemble were determined by close-to-real model spatial spectra of developed wind-generated waves which, in turn, were calculated with the help of known frequency spectra for a given characteristic wind velocity. The relationship between the new approach and traditional methods is demonstrated. Figures 3; references 8.

New Material for Acoustic Converters

917J0092D Moscow AKUSTICHESKIY ZHURNAL
in Russian Vol 37 No 2, Mar-Apr 91 pp 303-310

[Article by O. A. Kapustina, Acoustics Institute imeni N. N. Andreyev at the USSR Academy of Sciences]

UDC 534:535

[Abstract] Operating characteristics and service life of conventional acoustooptic (AO) liquid crystal (ZhK) converters and the factors affecting them are considered. The possibility of using new liquid crystal materials, such as nematic liquid crystals (NZhK) encapsulated in polymers which make it possible to eliminate the shortcomings of traditional converters and design devices with new functional features is examined. The new

material was made by applying a nematic liquid crystal emulsion in a polymer solution to a smooth surface; after the solvent evaporated, a polymer film with capsules filled with nematic liquid crystals was formed. The first results of an examination of the effect of ultrasound on the texture and optical properties of disperse nematic liquid crystal system encapsulated in a polymer matrix are cited and the characteristics of "dynamic" light scattering by this material and a pure homogeneous nematic liquid crystal sample are compared. Ways of improving operating characteristics of disperse systems and using the new materials for acoustooptic converters are discussed. Acoustic tests were carried out with emulsions developed by the "Monokristal-reaktiv" scientific production association in Kharkov. The results attest to the possibility of using the new materials in acoustooptic converters. It is shown that by using films with certain capsule dimensions and polymer matrix packing density, it is possible to attain the necessary contrast, sensitivity, and resolution of acoustooptic converters on the basis of the proposed materials. Figures 2; references 14: 7 Russian, 7 Western.

Nonlinear $m = 1$ Flute Mode Stability in Nonparaxial Open Confinement System

917J0097A Moscow FIZIKA PLAZMY in Russian
Vol 17 No 3, Mar 91 pp 309-315

[Article by I. M. Lanskiy, G. V. Stupakov, Nuclear Physics Institute at the Siberian Branch of the USSR Academy of Sciences]

UDC 533.951.2

[Abstract] Flute plasma mode stability to large displacements under the strong effect of finite Larmor ion radius is investigated by calculating the change in the plasma's potential energy during its displacement. It is shown that both the central confinement system and the stabilizer contribute to this change; the confinement system's contribution can be easily calculated since the magnetic field in it can be regarded as paraxial; the contribution is found to be negative, which corresponds to instability. Two configurations of stabilizing elements are considered: a plugging device and an anti-plugging device. A system consisting of a long axisymmetric plugging device with stabilizing cells located at its ends is considered. It is shown that depending on the type of stabilizer, the force returning the plasma to an equilibrium state may both increase (anti-plugging device) and decrease (nonparaxial plugging device) with an increase in displacement. For simplicity, only the energy of thin plasma shells from which any real pressure profile can be compiled was calculated. Figures 4; references 6: 5 Russian, 1 Western.

High-Frequency Surface Potential Waves on Metal's Boundary With Magnetoactive Plasma of Finite Pressure

917J0097B Moscow FIZIKA PLAZMY in Russian
Vol 17 No 3, Mar 91 pp 316-320

[Article by N. A. Azarenkov, K. N. Ostrikov, Kharkov State University imeni A. M. Gorkiy]

UDC 533.951

[Abstract] Surface waves localized near the interface of gaseous plasma and metal or in metallized semiconductor structures are considered; the waves' properties are determined by such plasma parameters as temperature and density and the external magnetic field. Allowing for the finite electronic subsystem pressure in the plasma, slow potential surface waves (PV) are possible in the system and propagate across the external magnetic field along the plasma/metal interface. The effect of transverse (to the wave propagation) plasma density irregularity on the variance of surface waves under study is investigated and variance equations of the waves under study in homogeneous and inhomogeneous plasma are derived. It is shown that electrostatic surface waves also exist in a frequency area where electromagnetic surface waves are impossible, i.e., the electron cyclotron frequency. As the irregularity parameter increases, the wave frequency decreases; thus, in the case of a high irregularity, the surface wave frequency domain becomes considerably more constricted and the waves may only be nonreciprocal. Figures 2; references 11: 8 Russian, 3 Western.

Nonlinear Electromagnetic Energy Emission by Surface Waves From Plasma Films of Variable Thickness

917J0097C Moscow FIZIKA PLAZMY in Russian
Vol 17 No 3, Mar 91 pp 321-326

[Article by A. A. Zharov, A. I. Smirnov, Applied Physics Institute at the USSR Academy of Sciences]

UDC 553.9

[Abstract] A thin plasma-like film with negative dielectric permittivity lying on the surface of perfect metal is considered. The effect of parametric emission of surface electromagnetic waves (PEV) from variable-thickness plasma films with cubic nonlinearity is investigated and it is shown that nonlinear surface electromagnetic wave emission from such films is characterized by a number of features, such as spatial localization of the glow area, a broad radiation pattern, etc. These phenomena are interesting from the viewpoint of nonlinear optical diagnostics of thin film coats. The competition among radiative and dissipative processes which results in the establishment of one of the two modes characterized by different ratios of radiated power to losses in the nonlinear interaction area is examined. The dependence of the emission efficiency on the effective nonlinear surface electromagnetic wave interaction area length is analyzed. It is noted that in principle, an opposite process is possible whereby energy from an incident volume wave is pumped into the surface electromagnetic wave. Figures 5; references 7: 4 Russian, 3 Western.

Investigation of Intense Electromagnetic Pulse Transit Through Vacuum Line With Plasma Jumper

917J0123A Moscow FIZIKA PLAZMY in Russian
Vol 17 No 5, Apr 91 pp 542-551

[Article by L. Ye. Aranchuk, V. M. Babykin, A. S. Chernenko, A. S. Chuvatin, Atomic Energy Institute imeni I. V. Kurchatov]

UDC 533.951

[Abstract] The use of plasma current interrupters (PPT), which makes it possible to control the output parameters of high-power electrophysical units, e.g., voltage, current, pulse duration and edge, and bremsstrahlung power and dose is discussed. An attempt is made to expand the base of experimental data on plasma current interrupters and suggest a workable model which would make it possible to trace the interruption stage and calculate energy losses. Experiments carried out in a magnetic system (MS) unit with a wave impedance of 2.3Ω where the incident wave has a 250 kV amplitude are described. The pulse-forming magnetic system is connoted to a stripline with a plasma current interrupter loaded into a diode. Electric and x-ray measurements and electron optical photography identified several characteristic interruption phases, e.g., wave processes on electrodes occurring at higher than Alfvén rates. It is shown that energy losses in the form of electron leakage are concentrated on the plasma jumper's diode boundary and are related to the lack of matching between various pulse transport segments. Experimental data make it possible to speculate that during the PPT interruption, processes develop not only in the transverse but also longitudinal direction whereby the electron leakage boundary may shift from the diode toward the generator and the ion leakage boundary—in the opposite direction. The use of PPT's made it possible to compensate for the effect of the tube inductance and load leads and operate at an output power closed to the matched condition. A model is developed which is based on representing the plasma region with the gap formed as a result of erosion by a vacuum line with an interelectrode boundary changing in time. The authors are grateful to V. D. Korolev for helping with experiments and A. V. Gordeyev for discussing the model. Figures 7; references 16: 6 Russian, 10 Western.

Particle Acceleration Under Effect of RF Field on Expanding Plasma

917J0123B Moscow FIZIKA PLAZMY in Russian
Vol 17 No 5, Apr 91 pp 552-559

[Article by S. V. Bulanov, I. N. Inovenkov, A. S. Sakharov, A. Ye. Chukhin, General Physics Institute at the USSR Academy of Sciences and Moscow State University imeni M. V. Lomonosov]

UDC 533.9

[Abstract] Phenomena accompanying the effect of intense laser or microwave (SVCh) radiation on plasma, such as scattering whose dynamics are largely determined by pondermotive forces, are summarized. The results of a numerical simulation of collisionless plasma in an intense RF field in the case of both plasma expansion into a vacuum and expansion into lower-density plasma are presented. The manifestation of two ion acceleration mechanisms—on the front of plasma expanding into a vacuum and in the plasma resonance region—is investigated in this formulation. Since real plasma virtually always contains a certain amount of impurities, plasma lightly doped with volatile ions which may be accelerated to energies greatly exceeding the fast ion energy of the main plasma components is considered in the simulation. The particle method is used in simulation. It is shown that fast ion acceleration during the RF field interaction with multicomponent plasma expanding into vacuum or lower-density background plasma may be attributed either to the energy accumulation by ions on the plasma/vacuum interface which is greatly enhanced by the fast electron generation in the plasma resonance vicinity or multivalent ion displacement from the plasma resonance area by RF pressure. Characteristic energies and energy spectra of accelerated ions in the resonance region are determined. The authors are grateful to V. A. Ivanov for constructive discussions. Figures 6; references 10: 8 Russian, 2 Western.

Experimental Study of Beam-Plasma Instability of Long-Pulse Monoenergetic Relativistic Electron Beam in Gas

917J0125A Moscow FIZIKA PLAZMY in Russian
Vol 17 No 4, Apr 91 pp 434-444

[Article by V. M. Batenin, V. S. Zhivopistsev, A. O. Ikonnikov, S. A. Ilchenko, A. T. Kunavin, A. V. Markov, D. V. Sapozhnikov, P. M. Tokar, V. Ye. Yakovlev, High Temperatures Institute at the USSR Academy of Sciences]

UDC 533.922

[Abstract] The development of various types of instability which accompany, and affect, the relativistic electron beam (REP) transport is discussed. In particular, radio-frequency electron-electron beam-plasma instability whose development is affected by the spread of beam particle velocities is considered. In so doing, kinetic and hydrodynamic modes are identified and their conditions are analyzed. The results of an experimental investigation of the beam-plasma RF electron-electron instability during the interaction of a long-pulse monoenergetic relativistic electron beam with a $\tau = 100 \mu\text{s}$ duration, a 300 keV energy, and 3-15 A current with nitrogen at a 0.02-8 torr pressure are presented. An electromagnetic valve was used to inject the beam into the gas. The experimental unit and techniques for taking electrophysical, optical, x-ray, and microwave (SVCh)

measurements are described. The relative electron velocity spread does not exceed 2×10^{-3} . The dependence of critical current (of the onset of instability) on the gas pressure and transport length is established. It is shown that a critical current increase with a beam transport length decrease is due to a feedback. The microwave plasma $\lambda = 8$ mm emission intensity distribution along the beam transport axis at $\tau = 20 \mu\text{s}$ is presented. Figures 7; tables 1; references 44: 35 Russian, 9 Western.

Intense Relativistic Electron Beam Propagation in Low-Density Plasma

917J0125B Moscow *FIZIKA PLAZMY* in Russian
Vol 17 No 4, Apr 91 pp 445-452

[Article by V. B. Krasovitskiy, O. Yu. Naguchev, S. I. Osmolovskiy, G. V. Fomin, Rostov State University]

[Abstract] The role of small ion addition to the relativistic electron beam (REP) in establishing radial equilibrium whereby the Coulomb repulsion force is compensated for

by the beam's own magnetic field is addressed. The propagation of an intense electron beam in low-density plasma and the ion channel formation are examined and the dynamics of charge neutralization of intense relativistic electron beams and ion channel development in low-density plasma are analyzed on the basis of the beam radius envelope equation. It is found that the excess electron charge field displaces "light" plasma electrons from the beam volume while "heavy" beam electrons are focused by the plasma ion charge; after plasma electrons are quickly displaced from the beam volume, radial Langmuir oscillations of the ion core with the trapped beam develop. A nonlinear theory of electron-ion instability caused by the beam motion in the ion channel and leading to spatial bunching of the system is proposed. The reciprocal effect of the surface wave field excited by the beam interaction with the electron shell surrounding the ion channel on the beam is analyzed. It is shown that the effect of electrostatic and electromagnetic instabilities on the beam depends on their relative increments. Figures 6; references 8.

Elevation of Thin-Film Superconducting Transition Temperature Due to Deposition of Normal Metal on Surface

917J0086B Moscow PISMA V ZHURNAL
EKSPERIMENTALNOY I TEORETICHESKOY
FIZIKI in Russian Vol 53 No 5, 10 Mar 91 pp 250-253

[Article by I. L. Landau, D. L. Shapovalov, and I. A. Parshin, Institute of Problems in Physics imeni P. L. Kapitsa, USSR Academy of Sciences, Moscow]

[Abstract] Considering that the superconducting transition temperature for thin metal or MoGe films which are amorphous at room temperature is lower for thinner films, owing principally to localization of electrons, an experimental study was made pertaining to change of the surface resistance due to deposition of a normal metal on such superconducting films. While deposition of another metal lowers the surface resistance and thus weakens the effect of localization in the normal state at temperatures above critical, a change of the film composition will change the critical temperature T_c and thus influence the surface resistance at temperatures below critical. Addition of a normal metal should lower the critical temperature T_c , except in the exotic case of the two metals forming a chemical compound with a higher critical temperature. Deposition of a normal metal will therefore have generally two competing effects, presence of atoms of a normal metal tending to lower the critical temperature and diminished localization of electrons tending to raise it. Experiments were performed with 1.6 nm thick and 1.8 nm thick bismuth films, which had been cold-deposited so as to form stable amorphous structures with a critical temperature $T_{c0} \approx 6.1$ K. On these films were deposited 0.8 nm thick, 1.8 nm thick, and 5.6 nm thick layers of silver, this normal metal known not to form superconducting compounds with bismuth and cold-deposited Bi-Ag mixtures known to have a critical temperature lower than that for pure bismuth. Some bismuth films of each thickness were left bare, for reference. Bismuth films and then silver layers were deposited from two different evaporators on a glass substrate with four platinum contact tabs at liquid-helium temperature for electrical resistance measurements by the current-voltage method. Two tests were then performed, first with bare bismuth films of each thickness for a determination their critical temperature from the temperature dependence of their electrical resistance and then with silver-coated bismuth films for a determination of the new critical temperature. The results indicate that the surface resistance of thin superconducting films is their principal characteristic which determines their critical temperature and that the latter can be raised appreciably by decreasing the surface resistance, even when this is done by adding a normal metal. Figures 3; references 10.

Elasticity, Strength, and Fracture Character of High- T_c $\text{YBa}_2\text{Cu}_3\text{O}_{7-x}$ Ceramics of Varying Density in 4.2-293K Temperature Range

917J0089A Kharkov FIZIKA NIZKIKH TEMPERATUR
in Russian Vol 17 No 1, Jan 91 pp 46-52

[Article by V. N. Kovaleva, V. A. Moskalenko, V. D. Natsik, S. N. Smirnov, V. T. Zagoskin, Yu. G. Litvinenko, Engineering Low Temperature Physics Institute

at the Ukrainian Academy of Sciences, Kharkov and Monokristal reaktiv scientific production association, Kharkov]

UDC 538.945

[Abstract] Experiments in quasistatic compression of high- T_c $\text{YBa}_2\text{Cu}_3\text{O}_{7-x}$ ceramics within the 4.2-293K temperature range carried out in order to investigate the patterns of strength behavior, static Young modulus, and fracture characteristics are described. Ceramics with a density varying within $\rho = 3.6 - 5.9$ g/cm³ were made from the same raw materials by the same technology. High- T_c 1-2-3 ceramics made by hot extrusion from a powder with a stoichiometric composition of $\text{YBa}_2\text{Cu}_3\text{O}_{7-x}$ prepared by solid phase synthesis using the carbonate technology were studied. The effect of porosity (the principal structural factor of ceramic materials) on their mechanical properties and fracture behavior is examined. A peculiar feature is detected in the dependence of strength on temperature in low-density ceramics in the 60-200K range; this feature correlates with anomalies of their acoustic characteristics. Physical mechanisms of low-temperature fracture and their relationship to the strength behavior patterns observed are analyzed. In a general case, mixed fracture corresponds to the most noticeable change in ultimate strength. The study was supported by the Scientific Council of the USSR Academy of Sciences on the problem of VTSP and was carried out in the framework of project No. 370 of the "High-Temperature Superconductivity" State Program. Figures 4; references 12: 8 Russian, 4 Western.

Temperature Anomalies of Yttrium Ceramics Impedance and Heat Capacity at $T \geq T_c$

917J0089B Kharkov FIZIKA NIZKIKH TEMPERATUR
in Russian Vol 17 No 1, Jan 91 pp 53-59

[Article by V. M. Dmitriyev, V. N. Yeropkin, A. M. Gurevich, A. P. Isakina, M. N. Ofitserov, N. N. Prentslau, A. I. Prokhvatilov, Engineering Low Temperature Physics Institute at the Ukrainian Academy of Sciences, Kharkov]

UDC 539.292

[Abstract] Anomalous temperature behavior of mechanical, thermal, electric, magnetic, or other properties of yttrium ceramics manifested as one, or a series of peaks, on the regular curve, breaks in the curve, as well as hysteretic phenomena is addressed. In order to determine these peculiarities and identify their origin, a cycle of measurements of the yttrium ceramics' impedance and heat capacity was taken in the $10^6 - 10^{10}$ Hz frequency band; in addition, x-ray studies of the same samples were carried out. Monophase $\text{YBa}_2\text{CuO}_{6.8}$ ceramics were used in the studies. Impedance was measured by the resonance method, anomalies were found

within the 82-85, 92-95, 155-165, 180-240, and 240-290K temperature ranges in the RF band. Heat capacity anomalies were also detected within these ranges. In addition to peaks, they were manifested as valleys in the temperature plots of these quantities as well as hysteretic phenomena. The origin of these peculiar features is discussed. The fact that DC resistive losses of ceramics under study exceed their AC resistive losses and that the difference between them decreases with an increase in frequency attests to the percolation type of DC conductivity. It is speculated that anomalous impedance and heat capacity curves point to the fact that phase and structural transitions affect the quasiparticle spectrum and are manifested in transport properties of high- T_c (VTSP) superconductors. The anomalies are quite diverse and related to the degree of oxygen ordering; in each specific case, special studies are necessary to ascertain their origin. Figures 4; references 21: 11 Russian, 10 Western.

Superconductivity Destruction by Optical Radiation in Nonequilibrium Resistive States and $\text{YBa}_2\text{Cu}_3\text{O}_{7-x}$ High- T_c Films

917J0091D Moscow *ZHURNAL EKSPERIMENTALNOY I TEORETICHESKOY FIZIKI in Russian Vol 99 No 3, Mar 91 pp 911-928*

[Article by P. P. Vysheslavtsev, G. M. Genkin, Yu. N. Nozdrin, A. V. Okomelkov, Applied Physics Institute at the USSR Academy of Sciences]

[Abstract] Experimental examinations of the effect of superconductivity breakup under the effect of optical radiation, and particularly the nonthermal (unrelated to the superconductor lattice heating) superconductor film response to external optical radiation at $T \approx T_c$ are summarized. The results of theoretical and experimental studies of the resistive response of thin $\text{YBa}_2\text{Cu}_3\text{O}_{7-x}$ high- T_c (VTSP) films under the effect of laser radiation are presented. Two types of relaxation time are identified in the response: short (≤ 10 ns) and long (> 10 μ s); it is shown that the latter is related to the heating of the superconductor lattice. It is also demonstrated that both equilibrium (i.e., thermal) and nonequilibrium processes each characterized by its relaxation time contribute to the response. Thermal and nonthermal response components depend differently on temperature, illumination intensity, and transport current in the film. The behavior of resistance in the superconductor's spatially inhomogeneous film related to the disbalance in the quasiparticle system is considered; it is shown that the change in the resistive state of an inhomogeneous superconductor is due to the superconductor penetration by electric current. The effect of "hot" quasiparticles may be interesting from the viewpoint of applications since characteristic settling and breakup times of the nonequilibrium state in the quasiparticle system may be very short (less than 10^{-12} s), making it possible to develop various fast electronic devices employing these effects. The authors are grateful to A. A. Andronov for useful discussions, Ye. B. Klyuyenkov, S. A. Pavlov, A. V. Varganov, Ye. V.

Pisarev, S. N. Ovchinnikov, T. A. Kuzmina, and I. N. Gavrilov for providing samples. Figures 12; references 25: 12 Russian, 13 Western.

Josephson Junction With Ferromagnetic Interlayer

917J0100C Moscow *PISMA V ZHURNAL EKSPERIMENTALNOY I TEORETICHESKOY FIZIKI in Russian Vol 53 No 6, 25 Mar 91 pp 308-312*

[Article by A. I. Buzdin and M. Yu. Kupriyanov, Moscow State University imeni M.V. Lomonosov, Moscow]

[Abstract] The characteristics of SFS Josephson sandwich junctions are analyzed, assuming that the material of both superconductor layers and the ferromagnetic interlayer material satisfy conditions of the "dirty" limit. Considering that the critical superconducting transition temperature for the ferromagnetic material is 0 K and its exchange field temperature is much higher than the critical temperature for the superconductor material in bulk form, typically within the 100-1000 K range, the dependence of the critical current on the thickness of the ferromagnetic interlayer is determined with the aid of Usadel's functions $F_{s,n}$ for both superconductor and ferromagnetic regions with respective coherence lengths and the diffusion coefficients taken into account. The system of four equations $F_{s,n}^{+/-} = F_{s,n}(\omega) + F_{s,n}(-\omega)$, where $\omega = \pi T(2m + 1)$ are Matsubara frequencies, is supplemented with the boundary conditions $F_{s,n}^{+/-} = F_n^{+/-}$ and $\sigma_s dF_{s,n}^{+/-}/dx = \sigma_n dF_n^{+/-}/dx$ (σ - electrical conductivity, x - coordinate across the sandwich) at the two F-S interfaces. Inasmuch as the boundary conditions for the F_n functions are independent of ω , the problem reduces to Ginzburg-Landau equations for superconductor electrodes with appropriate boundary conditions at the two F-S interfaces. The critical current is then found to be a damped nonnegatively oscillating function of both thickness and exchange field temperature of the ferromagnetic layer, periodically dropping to zero for sandwiches with ferromagnetic interlayers of a certain thickness and its multiples. Such a thickness dependence of the critical current is experimentally verifiable and analogous to its thickness dependence for SFS sandwiches whose materials satisfy conditions of the "pure" limit. Figures 3; references 9.

Theory of Superconducting SF and SFS Structures in Pure Limit at Temperatures Far Below Critical

917J0107A Moscow *TEORETICHESKAYA I MATEMATICHESKAYA FIZIKA in Russian Vol 86 No 2, Feb 91 pp 272-284*

[Article by S. V. Kuplevakhskiy, Kharkov State University, and I. I. Falko, Kharkov Polytechnic Institute]

[Abstract] A theory is constructed first for SF junctions (S - superconductor, F - ferromagnetic metal) and then for SFS sandwiches in the pure limit, to explain when

and how known anomalies at temperatures far below the critical one, namely Anderson quantization and change in the asymptotic behavior of the order parameter in the normal metal region, superpose on the effect of the exchange field which in this case negligible spin-orbital scattering reduces the order parameter to zero by inducing precession of the spins of both Copper pair partners. The theory is based on the quasi-classical Eilenberg equations, these equations being extended so as to account for the presence of an exchange field, while it also draws heavily on the known theory of pure superconducting SN and SNS structures. An order parameter is considered Gorkov's F-function of coincident arguments. Inasmuch as electrons with the most vigorous spin precession participate in the propagation of superconductivity correlations, these correlations cannot penetrate the ferromagnetic interlayer farther than some critical depth. For an SF junction is calculated the difference between its free energy the superconducting state and its free energy in the normal state, this difference being equal to minus the energy of an homogeneous superconductor plus an increment of energy due to the proximity effect and resulting suppression of Gorkov's F-function near the S-F or S-N boundary. For an SFS sandwich is calculated the excitation spectrum and, for one with a sufficiently thin ferromagnetic barrier layer, the possible existence of solitary polarized states of an Andreyev quasiparticle is predicted. The authors thank A. V. Svidzinskiy for very helpful discussion of the results. References 8.

Superconductivity in System of Electrons With Four-Fermion Tunneling Hamiltonian

917J0107B Moscow TEORETICHESKAYA I
MATEMATICHESKAYA FIZIKA in Russian Vol 86
No 2, Feb 91 pp 312-317

[Article by M. Ye. Zhuravlev and V. A. Ivanov, Institute of General and Inorganic Chemistry imeni N. S. Kurnakov, USSR Academy of Sciences]

[Abstract] Superconductivity of high- T_c superconductors is analyzed on the basis of the Hubbard-Hirsch model, which combines Hubbard's classical Hamiltonian and the tunneling Hamiltonian based on the Hirsch mechanism (J.E. Hirsch, PHYSICS LETTERS Vol A134, 1989) so that both intraatomic interaction of electrons and correlated interatomic hopping are taken into account. Considering that the estimated value of the interatomic energy exchange integral in cupric high- T_c superconductor compounds is within the $t = 0.1-1$ eV range, while $q = \text{mean}(|i|/|j|) = 0.5$ eV for hydrogen-like functions in the tunneling Hamiltonian; the Hubbard-Hirsch Hamiltonian and the energy of one-particle excitations are evaluated on a square t_p, q_p grid where $t_p = -2t(\cos p_x + \cos p_y)$ and $q_p = -2q(\cos p_x + \cos p_y)$ (p - momentum). The superconducting transition temperature T_c is calculated on the basis of the kinematic mechanism of high-temperature superconductivity (P.W. Anderson, SCIENCE Vol 235, 1987). It is

obtained from the anomalies of electron-electron scattering amplitudes in accordance with the Gorkov formalism, equivalent here to the condition for solvability of the system of homogeneous Bethe-Salpeter equations for four vertex parts, then in the logarithmic approximation presupposing that any one of the two ξ_{\pm} branches of the Fermi excitation spectrum vanishes at certain $t_p = t^*$ points. Both the effective interaction constant Λ and the superconducting transition temperature T_c are in this approximation shown to depend not only on t^* and n (number of electrons per node) but also on the ratio $\gamma = q_p/t_p = q/t$ ratio and the Hubbard correlation integral I . For noncorrelated electrons with four-fermion tunneling in the $\gamma \ll 1$ limit T_c varies as $e^{-1/2\gamma(1-n)}$, which corresponds to Bose condensation as a consequence of correlated hopping. In the atomic limit $\gamma \gg 1$ ($t = 0, q$ not 0, $I = 0$) T_c varies as $e^{-1/\Lambda}$ and superconductive electron pairing occurs when n is either within the $1/2 < n < 2/3$ range or within the $1 < n < (9 - 17^{1/2})/4$, which corresponds to the broken-line nonmonotonic dependence of the chemical potential μ on the number n . Superconductivity is thus possible under a negative chemical potential $\mu < 0$, but only within certain ranges of t^*, q , and I values. In these cases the expression for the equivalent interaction constant agrees with those based on the Hubbard model and on the Hirsch model (J.E. Hirsch, PHYSICS REVIEW B, Vol 39, 1989). Otherwise, correlated four-fermion tunneling of electrons complicates the phase diagram in the Hubbard model by breaking its electron-hole symmetry. The authors thank Yu. A. Zolotov for support and R. O. Zaytsev for valuable discussion. Figures 2; references 14.

Production of Thin Tl-Ba-Ca-Cu-O High- T_c Superconductor Films

917J0110B Leningrad PISMA V ZHURNAL
TEKHNICHESKOY FIZIKI in Russian Vol 17 No 6,
26 Mar 91 pp 61-64

[Article by O. R. Baydakov, V. N. Golubev, V. A. Yermakov, and Ye. V. Klyuyenkov, Institute of Applied Physics, USSR Academy of Sciences, Nizhny Novgorod]

[Abstract] Thin films of Tl-Ba-Ca-Cu-O high- T_c superconductor were deposited by the laser-beam sputtering process on SrTiO₃ and MgO substrates at 150-250° temperatures in an oxygen atmosphere under a pressure of 0.1 torr and subsequent annealing at 850°C temperature necessary for synthesis. Targets including the Tl₂Ba₂Ca₂Cu₃O₁₀ - δ compound and a controllable amount of the Tl₂O₃ oxide were treated with radiation pulses of 0.2 J energy and 10 ns duration at a repetition rate of 30 Hz from LTI-205 YAG:Nd³⁺ lasers. The amorphous films were variously annealed: 1) on a gold foil in a sealed quartz tube, 2) in a hermetic crucible made of stainless steel, 3) in a heater placed inside a vacuum chamber. This made it possible to determine the dependence of the superconducting transition parameters on the annealing conditions. The temperature dependence of their electrical resistivity was determined

on the basis of standard voltage drop measurements with a current of 100 μ A. Superconducting transition of 30 nm thick films on SrTiO_3 substrates began at 115-105 K temperatures and ended with an $R = 0$ resistance at 95-90 K temperatures. Superconducting transition of 30 nm thick films on MgO substrates began at 125-120 K temperatures and ended with an $R = 0$ resistance at 100-90 K temperatures, the higher temperatures of transition onset indicating presence of the $\text{Ti}_2\text{Ba}_2\text{Ca}_2\text{Cu}_3\text{O}_{10}$ - a but the wider $\Delta T = 15$ -20 K transition range indicating a higher degree of nonhomogeneity due to presence of other phases with weak links between crystals throughout the film volume. The critical current density for 1 mm wide and 1.3 mm long strips of these films was 1000 A/cm². Films with a smooth surface structure are difficult to obtain, because they melt during annealing at 850°C and then crystallize from the melt. In order to produce films with a smooth surface structure, it is therefore necessary to establish a temperature gradient normal to the surface of the melt so that crystallization will proceed from the substrate up. The conditions then are, however, thermodynamically less favorable for bulk crystallization. Figures 2; references 13.

Bisoliton Model of High- T_c Superconductivity: Review

917J0116B Kiev UKRAINSKIY FIZICHESKIY
ZHURNAL in Russian Vol 36 No 3, Mar 91
pp 401-419

[Article by A. S. Davydov, Theoretical Physics Institute at the Ukrainian Academy of Sciences, Kharkov]

UDC 537.312.62

[Abstract] Peculiar properties of superconductors are considered in the survey on the basis of the concept of the bisoliton model developed at the Theoretical Physics Institute at the Ukrainian Academy of Sciences in the wake of the pioneering discovery of the effect of superconductivity by Mueller and Bednorz in ceramic La, Ba, and Cu oxides at temperatures above 30K as well as successful attempts by Chu *et al* to synthesize yttrium compounds with $T_c \approx 90$ K. Gradual increases attained in the superconductor's critical temperature since the discovery of superconductivity by Kammerlingh Onnes in 1911, Bardin's, Cooper's and Schrieffer's (BKS) microscopic theory of superconductivity, superconductivity of metal oxides, principal properties of copper oxide superconductors, early theoretical investigations of the effect of high- T_c superconductivity (VTSP), a bisoliton model of ceramic oxide superconductivity, stability conditions of bisolitons, a quasiunidimensional model of ceramic oxide superconductivity and its justification, single-particle excitation in the bisoliton model, and Cooper pair breakdown in a static magnetic field are examined. Principal properties of a bisoliton Bose-condensate are identified and Meissner's effect in the bisoliton model is described. Figures 7; tables 2; references 25: 4 Russian, 21 Western.

On New Class of Normal Fermi-Fluids

917J0118A Moscow PISMA V ZHURNAL
EKSPERIMENTALNOY I TEORETICHESKOY
FIZIKI in Russian Vol 53 No 4, Feb 91 pp 208-211

[Article by G. Ye. Volovik, Theoretical Physics Institute imeni L. D. Landau at the USSR Academy of Sciences, Chernogolovka]

[Abstract] The general topological structure of Green functions is considered for Fermi-fluid systems in light of the ongoing discussion of the origin of high- T_c superconductivity in nontraditional states of Fermi-fluids. It is shown that Luttinger's and marginal Fermi-fluids belong to the same topological class as an ordinary Fermi-fluid, i.e., their Green function in a momentum space has a vortical singularity, while the locus in which the singularity is present forms the Fermi-surface. It is demonstrated that this vortical singularity is preserved with a transition to a marginal or Luttinger's Fermi-fluid but becomes transformed with a transition to a fermion condensate state in which the Fermi-surface is blurred, turning into a finite width Fermi-band (vortical leaf) which, by analogy to eddies in a superfluid liquid, corresponds to splitting of a vortex with one circulation quantum into two semivortices connected by a vortical leaf. The author is grateful to V. A. Khodel and C. J. Pethick for valuable discussions. Figures 2; references 8: 2 Russian, 6 Western.

Magnetization Characteristics of Highly Anisotropic Superconductors

917J0118B Moscow PISMA V ZHURNAL
EKSPERIMENTALNOY I TEORETICHESKOY
FIZIKI in Russian Vol 53 No 4, Feb 91 pp 212-223

[Article by N. V. Zavaritskiy, V. N. Zavaritskiy, Physics Problems Institute imeni P. L. Kapitsa and General Physics Institute at the USSR Academy of Sciences, Moscow]

[Abstract] The results of an investigation of high- T_c (VTSP) superconductor single crystal magnetization in fields which correspond to the onset of mixed state and structure genesis are presented. It is shown that in addition to a singularity which corresponds to the critical parallel magnetic field—eddy penetration along Cu-O crystal layers—there is an additional maximum on the $M(H)$ magnetization versus magnetic field plot of single crystals of stratified 123-YBaCuO and 2212-BiSrCaCuO superconductors (whose magnitude and position depend on the field slope) which corresponds to the eddy penetration perpendicular to the layers. Measurements of parallel and perpendicular magnetization components of superconductors with T_c of about 95K were taken in the 4.2-80K range after cooling the samples in a "zero" field in A. A. Yurgens's Nb-SQUID-magnetometer while measurements in the 77- T_c range—in a VTSP-SQUID magnetometer. The magnitude and temperature plot of the first critical field of Bi-2212 are determined. The authors are grateful to A. A. Yurgens for providing a

low-temperature VTSP magnetometer and to V. L. Pokrovskiy and A. A. Simonov for constructive discussions. Figures 3; references 18: 4 Russian, 14 Western.

Electron-Induced Light Scattering in Conducting High- T_c State

917J0121A Moscow PISMA V ZHURNAL
EKSPERIMENTALNOY I TEORETICHESKOY
FIZIKI in Russian Vol 53 No 7, Apr 91 pp 373-376

[Article by V. N. Kostur, G. M. Eliashberg, Theoretical Physics Institute imeni L. D. Landau at the USSR Academy of Sciences, Chernogolovka]

[Abstract] A number of unique features characterizing electron-induced light scattering (ERS) in various high- T_c (VTSP) compounds and in particular the considerable extent of the electron continuum in the continuous Raman scattering (KR) spectrum of cuprate metal oxides are discussed. It is shown that the phenomena determined by considerable attenuation comparable to the quasiparticle energy and lagging interaction called for reevaluating the classical approach to describing electron-induced light scattering in normal high- T_c superconductor state. The quasiparticle light scattering channel in high- T_c superconductors at $T \approx T_c$ is analyzed and the dependence of the electron-induced light scattering intensity on frequency is established. It is shown that light scattering by carriers interacting with phonons is characterized by a broad interval within which lag effects play a significant role. The authors are grateful to V. B. Timofeyev, A. A. Maksimov, and I. I. Tartakovskiy for discussing electron-induced light scattering experiments and V. A. Konyshov for help with numerical calculations; Mr. Kostur is grateful to V. G. Baryakhtar for support. Figures 2; references 8: 3 Russian, 5 Western.

On Temperature Dependence of Field Penetration Depth in Superconductors

917J0121B Moscow PISMA V ZHURNAL
EKSPERIMENTALNOY I TEORETICHESKOY
FIZIKI in Russian Vol 53 No 7, Apr 91 pp 381-382

[Article by G. V. Klimovich, A. V. Rylyakov, G. M. Eliashberg, Theoretical Physics Institute imeni L. D. Landau at the USSR Academy of Sciences, Chernogolovka]

[Abstract] Experimental and theoretical studies which speculate that at low temperatures ($T \ll T_c$), the dependence of the field penetration depth on temperature is exponential are discussed and it is shown that this phenomenon is a direct corollary of tight coupling equations in the presence of low-frequency excitation. In the tight coupling case under study, phonon corrections to the electromagnetic peak can be ignored since they do not contain perturbations and do not change the dependence of penetration depth on temperature. A more general examination of related phenomena in the future is suggested. References 4: 2 Russian, 2 Western.

Dependence of Bi-Sr-Ca-Cu-O:Pb Gap Parameter on Temperature

917J0124B Leningrad PISMA V ZHURNAL
TEKHNICHESKOY FIZIKI in Russian Vol 17 No 9,
May 91 pp 27-34

[Article by L. I. Leonyuk, M. V. Pedyash, D. K. Petrov, Ya. G. Ponomarev, Kh. T. Rakhimov, K. Setupati, M. V. Sudakova, A. B. Tennakun]

[Abstract] Attempts to measure the gap parameter Δ in S-I-S tunneling junctions and the gap's temperature function $\Delta(T)$ within a broad temperature range are summarized and efforts to develop good S-I-S junctions on the basis of high- T_c (VTSP) junctions with artificial and natural barriers are analyzed. In the experiment under study, a natural Schottky-type barrier developing on the break junction surface during the generation of a microcrack in single crystal Bi-Sr-Ca-Cu-O:Pb (2:2:1:2-phase) samples at liquid helium temperatures was examined in order to determine the temperature dependence of their gap parameter. To this end, thin single crystal wafers with reflecting surfaces and 2x2 mm cross-sectional dimensions were sliced off by a blade from the ingot. The microcrack onset was detected by a drop in the critical supercurrent to several tens of microamps; the gap parameter at $T = 4.2K$ was found by Dynes's method. The $\Delta(T)$ function was determined with a broad $4.2K < T < T_c$ temperature range; the results obtained in a number of single crystals are consistent with each other and are adequately described by the Bardeen-Cooper-Schrieffer (BKS) formal theory. Figures 3; tables 1; references 12: 2 Russian, 10 Western.

On Physical Origin of Superconducting Polar Elastomer Channels

917J0128A Leningrad PISMA V ZHURNAL
TEKHNICHESKOY FIZIKI in Russian Vol 17 No 10,
May 91 pp 45-50

[Article by L. N. Grigorov, Synthetic Polymer Materials Institute at the USSR Academy of Sciences, Moscow]

[Abstract] An attempt is made to clarify the physical origin of the long (0.1 mm) conducting channels of small diameter of $d \leq 10$ nm which form during the oxidation of rubbery polymers and combine an abnormally high conductivity of $>> 10^{11} (\Omega \cdot \text{cm})^{-1}$ with ferromagnetism. To this end, a model of such compounds is considered allowing for the fact the mobile dipole groups form in the elastomer, thus leading to a low ratio of high- and low-frequency permittivity of the medium ($<< 1$). It has been established that as a result, some of the elastomer's functional groups become easily ionized, so static ions and low-mobility polarons accumulate in the polymer. The elastomer medium is assumed to be a continuum for polarons. It is shown that in the channeling conduction

model, ferromagnetic electron organization is more efficient than diamagnetic; the model explains both the appearance of highly anisotropic local conduction in polar elastomers and the simultaneous ferromagnetism. Figures 1; references 11: 10 Russian, 1 Western.

Effect of $\text{YBa}_2\text{Cu}_3\text{O}_{7-x}$ Superconducting Metal Oxide Doping With Boron Nitride on its Properties

917J0129B Leningrad PISMA V ZHURNAL
TEKHNICHESKOY FIZIKI in Russian Vol 17 No 8,
Apr 91 pp 20-26

[Article by Ye. M. Gololobov, I. I. Papp, N. A. Prytkova, Zh. M. Tomilko, D. M. Turtsevich, N. M. Shimanskaya, Solid State and Semiconductor Physics Institute at the Belorussian Academy of Sciences, Minsk]

[Abstract] Practical applications of high- T_c superconductors (VTSP) in cryomicroelectronic devices, whose functional properties are largely determined by the high- T_c superconductor film junction with the substrate, and the importance of preventing their atomic interdiffusion

from seriously affecting the superconducting film parameters are discussed. The results of a study of yttrium high- T_c superconductor interaction with boron nitride are presented. To this end, $\text{YBa}_2\text{Cu}_3\text{O}_{7-x} + \text{BN}$ compositions were prepared in the (1:2:3) + BN_x ratio by synthesizing finely dispersed powders by the solid phase reaction method at a 700-710°C temperature for 42 h in the air at a 400K/h heating rate and 50 K/h cooling rate. Sintering was performed at 950°C for 1h 15 min. The samples' phase composition was determined by a DRON-3 x-ray diffractometer in CuK_α radiation. X-ray diffraction curves and the temperature dependence of $R(T)/R$ of samples doped with boron nitride in the amount of $0 \leq x \leq 3.0$ at 300K are plotted and the values of critical temperature initial, final, and mid points, as well as range as a function of composition are analyzed. The study shows that for making thin-film yttrium high- T_c superconductors allowing for boron nitride's ability to facilitate the Y_2BaCuO_5 phase formation, the most suitable are boron nitride substrates coated with a buffer layer of $\text{YBa}_2\text{Cu}_3\text{O}_{7-x}$ doped with BN or Y_2BaCuO_5 . Figures 2; tables 1; references 12: 4 Russian, 8 Western.

On New Trend in Microelectronic Magnetic Storage Device Technology

917J0124C Leningrad PISMA V ZHURNAL
TEKHNICHESKOY FIZIKI in Russian Vol 17 No 9,
May 91 pp 34-37

[Article by A. N. Averkin, V. P. Dmitriyev]

[Abstract] The early experimental results of efforts which represent a new trend in microelectronic magnetic recording technology are cited and briefly substantiated. Thin-layer strips of magnetic uniaxial material whose light magnetization axis (OLN) is perpendicular to the strip plane with a periodically varying width (i.e., a sequence of wedges) was used as the information medium. The domain boundary (DG) position in the strip loci where their energy is minimal and the domain boundary motion under the effect of a uniform magnetic

field parallel to the light magnetization axis are examined. From the viewpoint of dynamic characteristics, the wedge-shaped domain phase sequence structure is phenomenologically represented as a structure with artificial anisotropic coercivity (SIAC) characterized by different starting fields in two different domain wall movement directions, thus making it possible to control the domain wall motion in the forward and backward directions. The above magnetic structures can be used as data media if the presence of open domain walls (NDG) in the structure locus is defined as "1" while its absence, as "0" (in a binary code). Thus, the essence of direction amounts to using SIAC structures which are characterized by a metastable monodomain state and anisotropy of parameters which determine its dynamic characteristics, thus making it possible to store and move information. The authors are grateful to L. A. Suslin for constant interest in the effort. Figures 1; references 1.

New Approach to Problem of Detecting Gravitational Waves

917J0101B Moscow PISMA V ZHURNAL
EKSPERIMENTALNOY I TEORETICHESKOY
FIZIKI in Russian Vol 53 No 6, 25 Mar 91
pp 1122-1125

[Article by A. B. Balakin, G. V. Kisunko, corresponding member, USSR Academy of Sciences, Z. G. Murzakhanov, and N. N. Rusyayev, Department of Theoretical Problems at USSR Academy Sciences, Moscow, Kazan State University imeni V. I. Ulyanov-Lenin, and Kazan Institute of Aviation imeni A. N. Tupolev]

UDC 537.867+523.034.43

[Abstract] A new method of detecting gravitational waves is proposed which offers a solution to the problem of using laser-interference detectors with a very long vacuumized optical base, namely use of active optical ring cavities operating in the recirculation mode and thus retaining the modulation of optical radiation by the field of a gravitational wave. In a cavity with a time constant of the order of 1 s it should thus be possible to compensate electrical losses over an optical path in the active medium of up to 3×10^8 m equivalent length. Parametric action of a periodic gravitational wave on such a cavity should, moreover, make nonlinear amplification of that modulation effect possible under conditions of parametric resonance in a cavity with the optimum active medium and the optimum configuration. High detector sensitivity and selectivity can thus be

ensured, on the premise that periodic gravitational waves are emitted by reliably predictable sources such as relativistic astrophysical twin systems of the PSR 1913 + 16 kind. The new concept is validated theoretically on the basis of a simple mathematical model describing the nonlinear effects of parametric action of the field of a periodic gravitational field on the electromagnetic field in an active cavity. The model consists of two Maxwell field equations with boundary conditions for a given cavity configuration and initial conditions in the absence of a gravitational wave, two metrics of a plane gravitational wave, and a system of equations relating the two electromagnetic field tensors to the model optical properties of the active medium in the linear approximation. With the aid of these and the Maxwell field equations are formulated equations of the 4-potential evolution. These equations are solved without the constraints of geometrical optics and of a weak gravitational wave, thus considering such a nonlinear wave in vacuum. Analysis of the solution reveals that the field of a periodic gravitational wave indeed modulates the amplitude, the phase, the polarization, the wave vector, and the Poynting vector of an arbitrarily oriented and arbitrarily polarized initially plane electromagnetic wave. Considering that phase modulation is preferred for detection of gravitational waves, for periodic gravitational waves in this case the Maxwell field equations can be reduced to a system of Hill equations. Phenomenological analysis of the action of a gravitational wave on condensed media with spatial symmetry of any of the 3m, 3m, 32, m3m, ∞ , ∞ m classes then confirms the possibility of parametric resonance in such a detector. References 6.